APL/JHU
CP 055
APRIL 1977



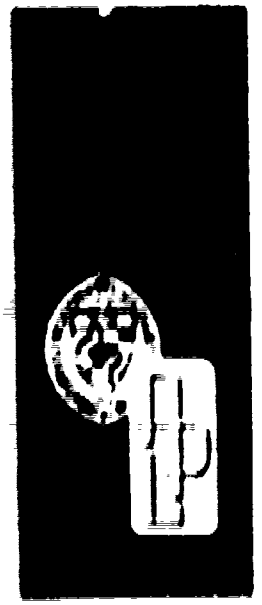

Space Systems

# THE APL MAGSAT ATTITUDE TRANSFER SYSTEM CONCEPT

I W SCHLNKLL
A TINKLL



THE JOHNS HOPKINS UNIVERSITY • APPLIED PHYSICS LABORATORY

| BIBLIOGRAPHIC DATA SHEET | 1. Report No. APL/JHU CP 055 | 2. | 3. Recipient's Accession No. |
|---|---|---|---|
| 4. Title and Subtitle<br>THE APL MAGSAT ATTITUDE TRANSFER SYSTEM CONCEPT | | | 5. Report Date<br>April 1977<br>6. |
| 7. Author(s)<br>Fred W. Schenkel, Abraham Finkel | | | 8. Performing Organization Rept. No. CP 055 |
| 9. Performing Organization Name and Address<br>The Johns Hopkins University Applied Physics Laboratory<br>Johns Hopkins Road<br>Laurel, MD 20810 | | | 10. Project/Task/Work Unit No.<br>Task X7T2<br>11. Contract/Grant No.<br>N00017-72-C-4401 |
| 12. Sponsoring Organization Name and Address<br>The Johns Hopkins University Applied Physics Laboratory<br>Johns Hopkins Road<br>Laurel, MD 20810 | | | 13. Type of Report & Period Covered<br>14. |

15. Supplementary Notes

16. Abstracts

This document describes the conceptual design and analysis for an Attitude Transfer System (ATS) to perform continuous measurement of the three-axis attitude of a vector magnetometer experiment, relative to a pair of star sensors fastened to a satellite body. The magnetometer is suspended at the end of a 20-ft boom extending from the body of MAGSAT (a survey satellite for measurement of the earth's magnetic field). A common optical bench serves as the mounting reference for both the ATS and the star sensors. The directional accuracy of the vector magnetometer experiment is required to be 20 arc seconds in all three axes. An error allocation analysis has determined that the ATS must provide an accuracy of 7 arc seconds per axis to meet the overall system requirements.

17. Key Words and Document Analysis. 17a. Descriptors

Satellite attitude
Magnetometers
Attitude control
Spacecraft guidance

17b. Identifiers/Open-Ended Terms

MAGSAT

17c. COSATI Field/Group 2201

| 18. Availability Statement | 19. Security Class (This Report) | 21. No. of Pages |
|---|---|---|
| Unlimited distribution | UNCLASSIFIED | 52 |
| | 20. Security Class (This Page) UNCLASSIFIED | 22. Price |

APL/JHU
CP 055
APRIL 1977

*Space Systems*

# THE APL MAGSAT ATTITUDE TRANSFER SYSTEM CONCEPT

F. W. SCHENKEL
A. FINKEL



THE JOHNS HOPKINS UNIVERSITY ■ APPLIED PHYSICS LABORATORY
Johns Hopkins Road, Laurel, Maryland 20810

THE JOHNS HOPKINS UNIVERSITY
APPLIED PHYSICS LABORATORY
LAUREL, MARYLAND

## ABSTRACT

This document describes the conceptual design and analysis for an Attitude Transfer System (ATS) to perform continuous measurement of the three-axis attitude of a vector magnetometer experiment, relative to a pair of star sensors fastened to a satellite body. The magnetometer is suspended at the end of a 20-ft boom extending from the body of MAGSAT (a survey satellite for measurement of the earth's magnetic field). A common optical bench serves as the mounting reference for both the ATS and the star sensors. The directional accuracy of the vector magnetometer experiment is required to be 20 arc seconds in all three axes. An error allocation analysis has determined that the ATS must provide an accuracy of 7 arc seconds per axis to meet the overall system requirements.

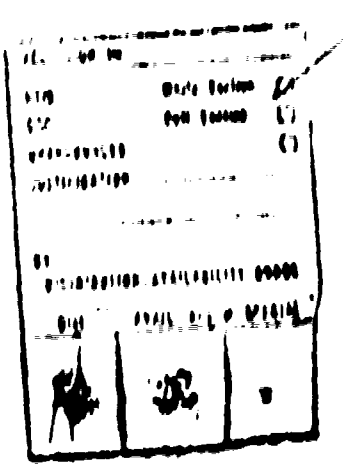

CONTENTS

## ILLUSTRATIONS

# 1. INTRODUCTION

Several design concepts for an Attitude Transfer System (ATS) have been explored from the standpoint of basic feasibility. They include the use of imaging sensors, point detectors, and quadrant detectors in conjunction with Lambertian, collimated, and coherent source signals as applied to imaging, collimated, grating, spinning-reticle, and polarized-light systems. Most concepts were discarded because of inadequate angular sensitivity, excess size or weight, overly complex large optics, moving components, etc.

The power requirements of the ATS are nominally modest. No specific restriction has been placed on power; something less than 2 W is expected to be adequate. However, it is imperative that no high-current demands be imposed by any system component that may be located in the vicinity of the magnetometer experiment. The residual magnetic field strength must be maintained below 1 gamma ($10^{-5}$ Oersted).

The data rate requirement for the magnetometer experiment is two per second; therefore, that is the lower limit of the data rate for the ATS. If required, the ATS can function with a kilohertz data rate. The data rate will be compatible with the sampling interval set by the telemetry for the experiment.

Materials used for component parts or to support component parts on or near the experimental package must be nonmagnetic. The total weight of the ATS should not exceed 10 lb. It is desirable to locate the sensing portion of the ATS near the stellar attitude measurement system on the satellite to minimize errors resulting from distortions in the structure separating such instrumentation. A common optical bench structure is required.

The ATS must be able to function with a 20-ft-long boom over a dynamic range in magnetometer-platform displacement motion of ±0.25° in any transverse direction. The dynamic range of twist motion measurement is to be a minimum of ±0.083°.

The mechanical design of the boom and the method of fastening it to the satellite on one end and to the experiment platform on the other limit the magnitude of angular motion of the experiment relative to the satellite body. The limits of distortion in the boom are shown in Fig. 1.

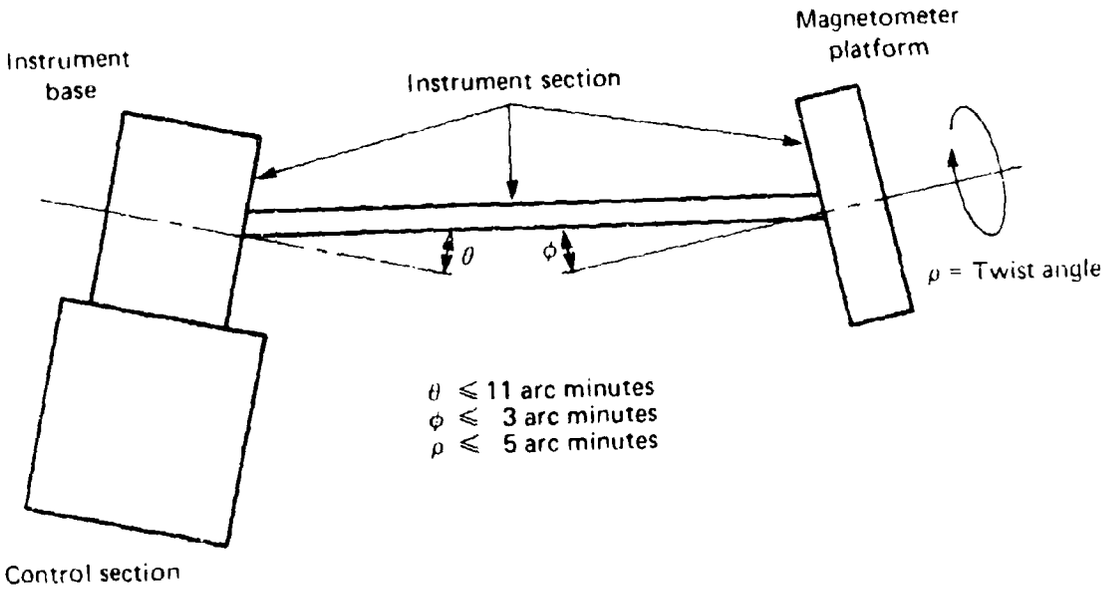


**Fig. 1 Maximum Allowable Misalignments for MAGSAT for Pitch and Yaw**

## 2. OBJECTIVES AND GOALS

The ATS is required to yield an accuracy of 7 arc seconds in all three axes. However, a goal has been set of 1 arc second for pitch/yaw and 5 arc seconds for twist. The pitch/yaw system will have an acquisition range of ±0.5° as a goal, with a precision range over ±3 arc minutes. The twist system will have a precision range of ±0.08° over the pitch/yaw precision range. The ultimate accuracy of each instrument depends mainly on the thermomechanical integrity of its optical components. It is anticipated that electro-optical error contributors will not be dominant. The ultimate accuracy of the total system depends on the thermomechanical integrity of the optical bench that serves as a common mounting platform for the ATS and the star sensor cameras. The extremely close tolerance requirements imposed on the optical bench are discussed in subsequent paragraphs. Because of these severe requirements, the ATS, the star sensor system, and the optical bench must be treated as a unit if such accuracy is to be achieved.

The ATS is intended to be immune to extraneous glint inputs. In addition, electro-optical equalization of each signal channel of a detector pair in any axis is mandatory.

# 3. ATTITUDE TRANSFER SYSTEM

This concept for a precision ATS uses proven techniques. All active components are located on the satellite body. The magnetometer instrument platform is equipped with two passive optical reflectors. There are no moving components and power consumption is low. Immunity from solar damage and glint as well as signal-source redundancy are provided. Automatic self-calibration and sensor equalization are built-in. Arc-second precision is provided over a range of ±3 arc minutes, with a projected acquisition capability of ±0.5° in pitch and yaw. It is proposed and is deemed mechanically feasible to provide the extender boom base with a dual-axis (±2.5°) motor-drive platform to place the ATS within its high-precision range when the boom is erected initially.

During the boom-erection phase the pitch/yaw sensor package of the ATS can be active. That will provide coarse angular tracking and facilitate simple attitude correction via the boom gimbal as required to locate the magnetometer instrument package within the ATS high-precision range. The twist sensor package will become operable after the pitch/yaw system is in the high-precision operating range. Figure 2 illustrates the layout of the three-axis ATS.

## CONCEPTUAL DESIGN

The basic precision measurement of pitch and yaw angular orientation is accomplished by means of an autocollimation technique using a flat mirror attached to the magnetometer instrument package (Fig. 2). Twist is measured by means of a split transmitter/receiver package where the optical beam is reflected from a dihedral mirror affixed to the magnetometer instrument package (Fig. 2). The attitude for each axis will be measured using intervals of a pulsed optical beam at a rate of approximately 10 kHz. Alternating with these intelligence signal intervals will be an internal-instrument, pulsed, optical calibration beam. The electronic signal processing and automatic calibration techniques are discussed in subsequent paragraphs.

Solar-damage immunity is accomplished by using PIN silicon diode detector elements throughout. Glints producing false intelligence signals or causing sensor saturation are avoided by means of pulsed, synchronously demodulated signals that are optically (spectrally) narrowbanded by 50-nm-wide dichroic filters. Such

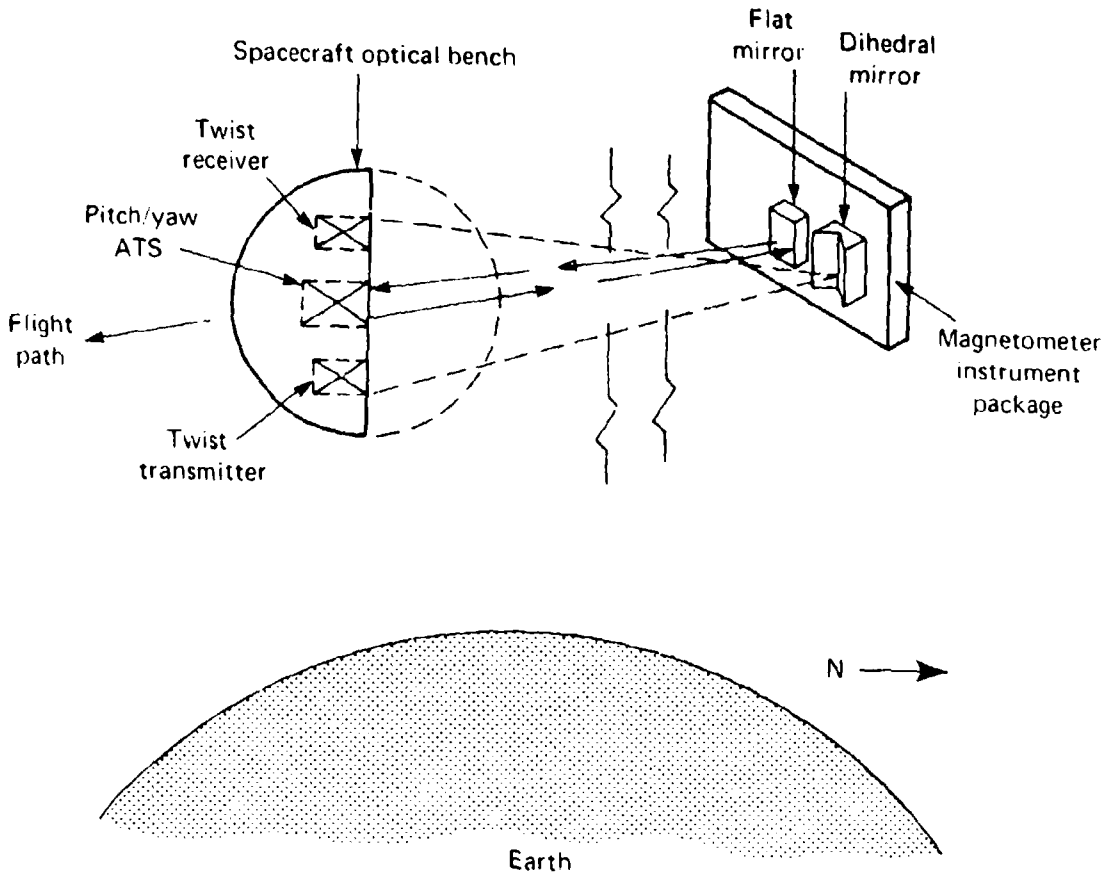


**Fig. 2 Layout of Attitude Transfer System**

filters reject approximately 97% of the solar spectrum. In addition, instrument sunshades will be provided if necessary. Inspection of the judicious instrument layout in the spacecraft and the orbit configuration shows that the entrance of glint signals into the ATS sensors is rather unlikely, as illustrated in Fig. 3. The minimum solar angle of 60° to the ATS will occur only during summer solstice.

## Electro-Optics

### Pitch/Yaw System

Figure 4 is a schematic of the pitch/yaw optical system. A collimated beam originating at a square aperture source is transmitted to a flat mirror on the magnetometer instrument package at a distance of 20 ft. The mirror is approximately 4.5 in. in diameter to handle the boom translation effects out to ±0.5°. The reflected beam is passed through the common transmit/receive (projection/objective) optic, through a half-silvered mirror splitter, and onto the receiver portion of the instrument.

The receiver optic, beyond the common projection/objective optic, takes the form of a mirrored pyramid splitter. The return optical image will be square, like the square reticle source at the transmitter. The mirrored receiver pyramid splits the image into four segments, all of which are used for both pitch and yaw computations. If the flat mirror on the magnetometer instrument package is truly orthogonal to the transmitted optical beam, the four segments of the return image on the mirrored pyramid will be equal. If the pitch or yaw (or both) of the magnetometer instrument package drifts from the boresight condition, the four segments will be unequal. This can be envisioned as a physical shift of the return image across the apex of the mirrored pyramid.

The change in size of the image segments results in a change in the optical signal level at the face of each of the four detector sensors. A condenser optic, which intervenes the optical path between each of the four mirrored faces of the pyramid and its respective detector, converts a change in the image segment size to an equivalent change in intensity of the optical signal on the detector. It is mandatory that the same area on the detector surface receive the incoming radiation, regardless of the angle of the incoming rays from the mirrored pyramid splitter, because of nonuniformities in sensitivity across the detector surface. Such nonuniformities would result in intolerable errors in attitude measurement. The use of a condenser optic overcomes this potential error.

The individual detectors are basically PIN silicon diode point detectors approximately 1 $mm^2$ (HP-5082-4207).

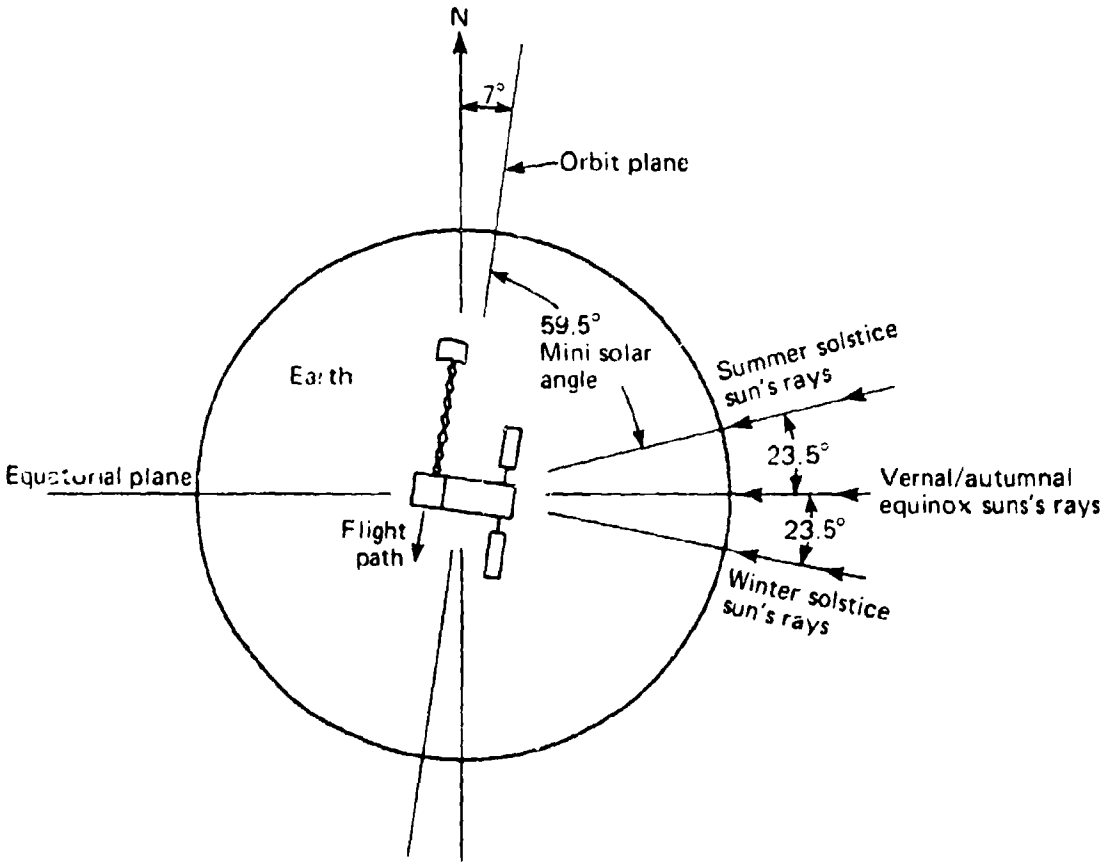


**Fig. 3 Spacecraft/Earth/Sun Orientation (morning launch)**

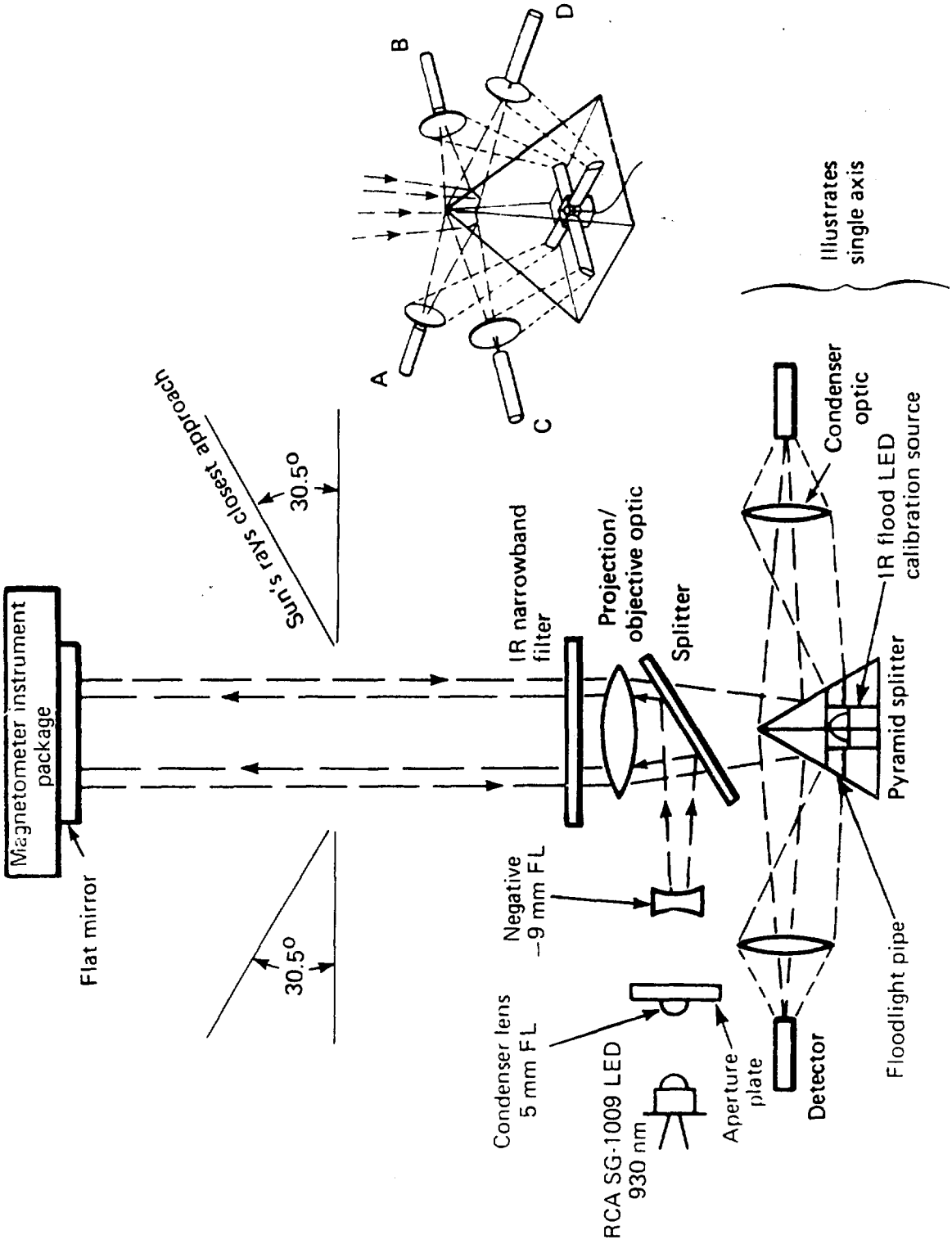


Fig. 4 Schematic of Pitch/Yaw Optical System

Figure 5 is a plan view of the mirrored pyramid with the optical image superimposed. The pyramid is rotated 45° with respect to the pitch/yaw error signals. Each segment of the split optical image remains square or rectangular. The pitch or yaw computation is indicated in Fig. 5. Figure 6 gives a sample computation for an angular change in either pitch or yaw attitude. An angular change of 1 arc second corresponds to a change in optical or electrical signal differential of 1 part in 180, which is very manageable.

Returning to Fig. 4, it may be observed that a calibration source using an IR flood beam LED (light emitting diode) is incorporated into the receiver section of the instrument, For clarity, the source is shown at an exaggerated distance from the optic axis. A common calibration source is used to illuminate all four detector channels of the instrument equally, the purpose being to equalize the individual detector channels relative to one another. This significant feature helps eliminate pitch/yaw measurement errors resulting from changes in individual channel sensitivity and/or amplifier gain. The optical calibration signal is injected into the receiver optical train so as to cover the same detector-sensitive area that is covered by the optical intelligence signal. It is also possible to include the mirrored pyramid in the optical calibration path by injecting the calibration flood beam through the pyramid apex. This eliminates errors due to possible unequal changes in the reflectivity of mirrored facets of the pyramid.

The use of a mirrored pyramid splitter in lieu of half-silvered mirror splitters reduces the instrument parts count and increases the level of the detected signal by 3 dB. A reduction in parts count is significant in that it reduces the number of critical alignments within the instrument.

The narrowband IR filter on the instrument is centered around 930 nm to accommodate the narrowband LED IR source (RCA SG-1009). A GaAs:Si doped LED is recommended for greater output stability. This spectral filter reduces to a very low level any extraneous glint sources of radiant energy that might enter the instrument. It also helps control thermal balance within the instrument.

The differential signal-to-noise ratio for the pitch/yaw system has been computed to be 78 dB. The detailed computations are in Appendix A.

Twist (Roll) System

Figure 7 illustrates the optical geometry for measuring twist. A dihedral mirror mounted to the magnetometer causes a twist angular multiplication twice that of a single-element mirror.

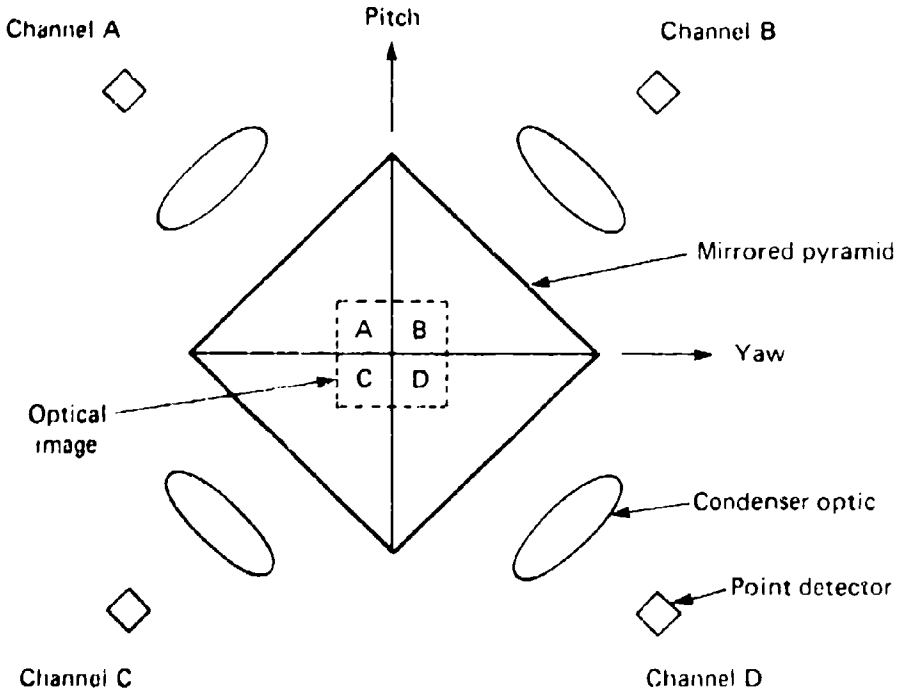


$$\text{Pitch} = \frac{(A+B) - (C+D)}{A+B+C+D} \qquad \text{(normalized)}$$

$$\text{Yaw} = \frac{(A+C) - (B+D)}{A+B+C+D} \qquad \text{(normalized)}$$

**Fig. 5 Optical Image Superimposed on Pyramid Splitter**

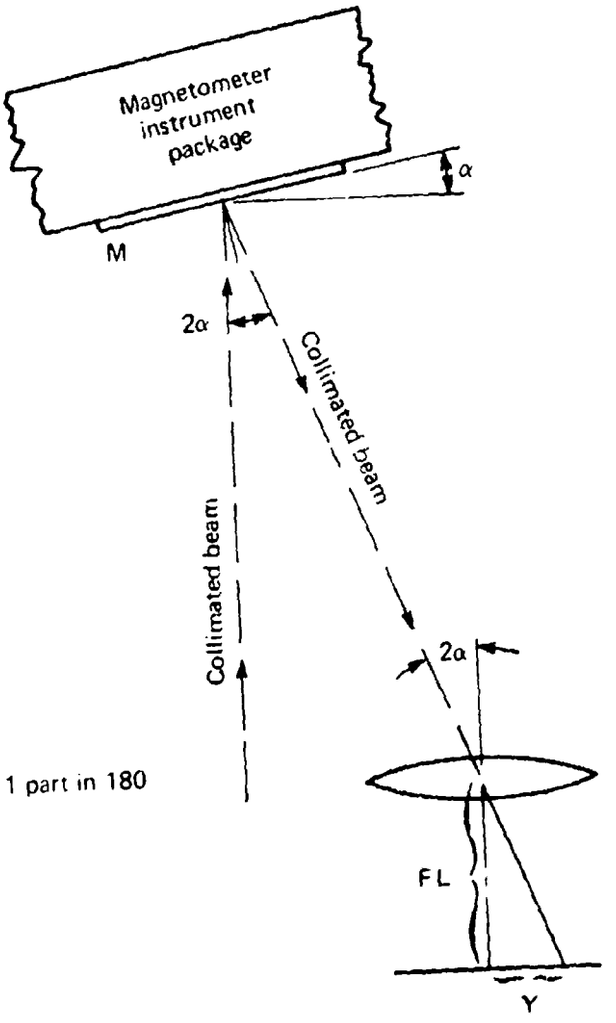


For $\alpha$ = 1 arc second = $5 \times 10^{-6}$ rad
FL = 8 in.
Image plane displacement:
$Y = 2\alpha(FL) = 8 \times 10^{-5}$ in.

Optical image

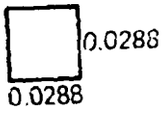


Signal incremental change or 1 arc second
(2 detector elements)

$$2\left(\frac{(8)10^{-5}\,(2.88)10^{-2}}{(2.88 \times 10^{-2})^2}\right) = 5.55 \times 10^{-3} \text{ or 1 part in 180}$$

Signal incremental change for 5 arc seconds
or 1 part in 36

**Fig. 6 Optical Geometry for Measuring Pitch and Yaw**

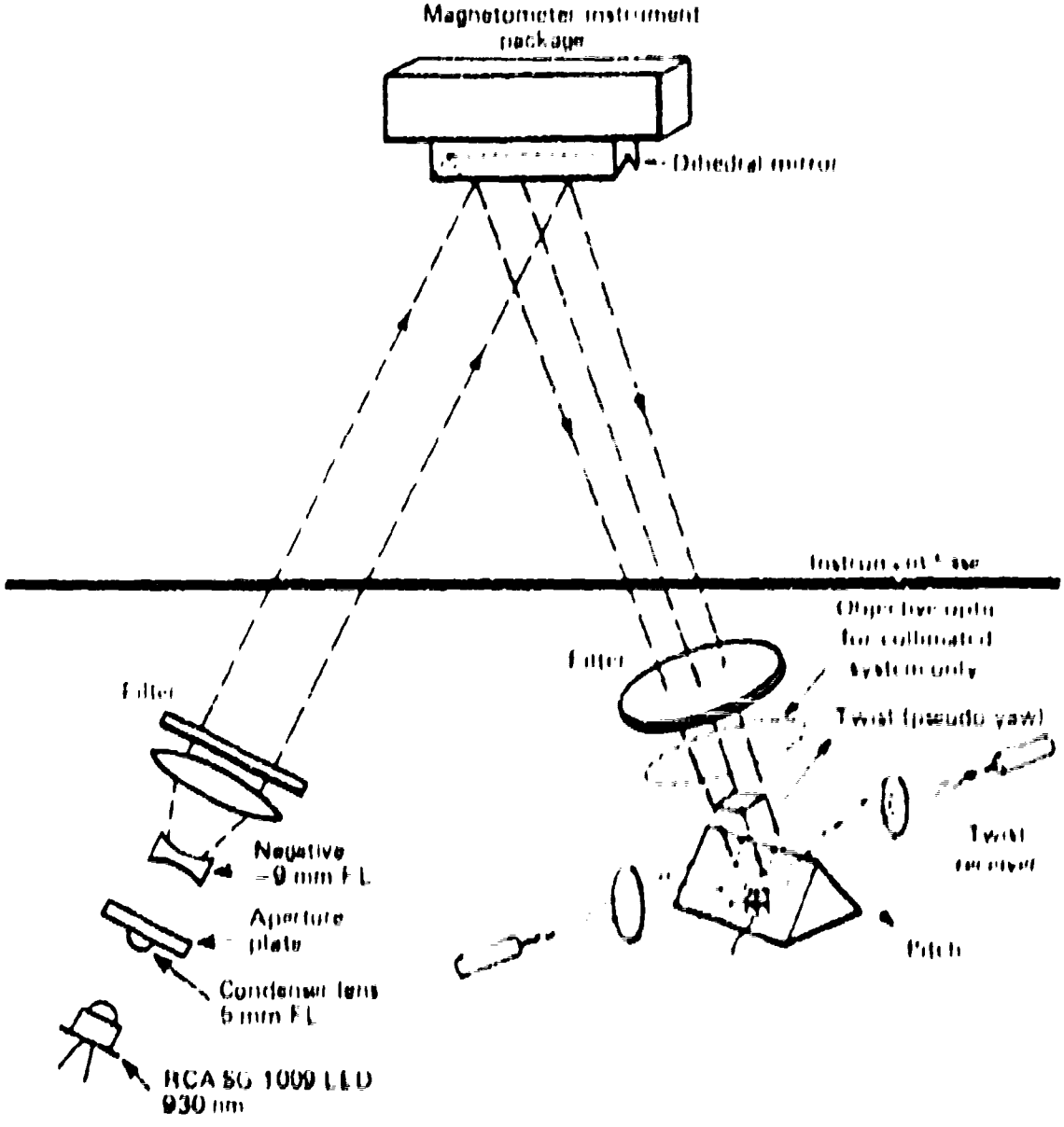


Fig 7 Focused Twist Sensor

It also decouples the twist measurement from yaw sensitivity for a vertically placed system (see Fig. 2). Appendix B gives a mathematical analysis of the roll-axis measurement transfer into a yaw motion, and of the yaw-axis immunity provided by the dihedral mirror for angles of less than 1°.

In Fig. 7, the instrument shown for measuring twist uses a focused optical beam. It could also use a collimated optical beam; however, that would require an objective optic in the receiver. Whether a focused or a collimated system is used will be determined as a result of the thermomechanical stability design trade-offs on the instrument module optical bench. The stability requirements for each approach are listed in Section 3. Appendix C gives the detailed geometric design considerations for both a collimated system and a focused system. The focused system offers the possibility of somewhat greater twist sensitivity and is used as a reference in this discussion.

The instrument for measuring twist, shown in Fig. 8, is similar in design to the pitch/yaw system, except for its having a split transmitter/receiver. A radiation source with a square cross section is transmitted to the dihedral mirror on the magnetometer instrument package and reflected back to the receiver. The square focused image is split by the mirrored prism; corresponding signals are reflected to individual silicon diode point detectors via the respective condenser optics. Here, as in the pitch/yaw sensor, the condenser optics provides optical signal equalization. The transmitter radiation source takes the form of an LED feeding a light-pipe condenser or a lens condenser. The light-pipe approach could use either a fiber optic splitter or a partially reflective mirror for redundant optical source injection. The spectral filters aid in thermal control in addition to ensuring glint rejection.

The focused twist sensor will be required to detect a change of 1 part in 1380 per arc second in the location of the square image on the mirrored prism, corresponding to an equivalent intensity change at the detectors. It must be remembered that the condenser optics in the receiver converts positional change in the image to intensity change at the individual detectors. The instrument signal-to-noise ratio is calculated to be 85 dB for a resolution of 5 arc seconds (see details in Appendix A).

Electronic Signal Processing

Because of the extreme accuracy required, the electronic system is designed to be insensitive to variations in LED output, detector response, and amplifier gain. Active control is used in

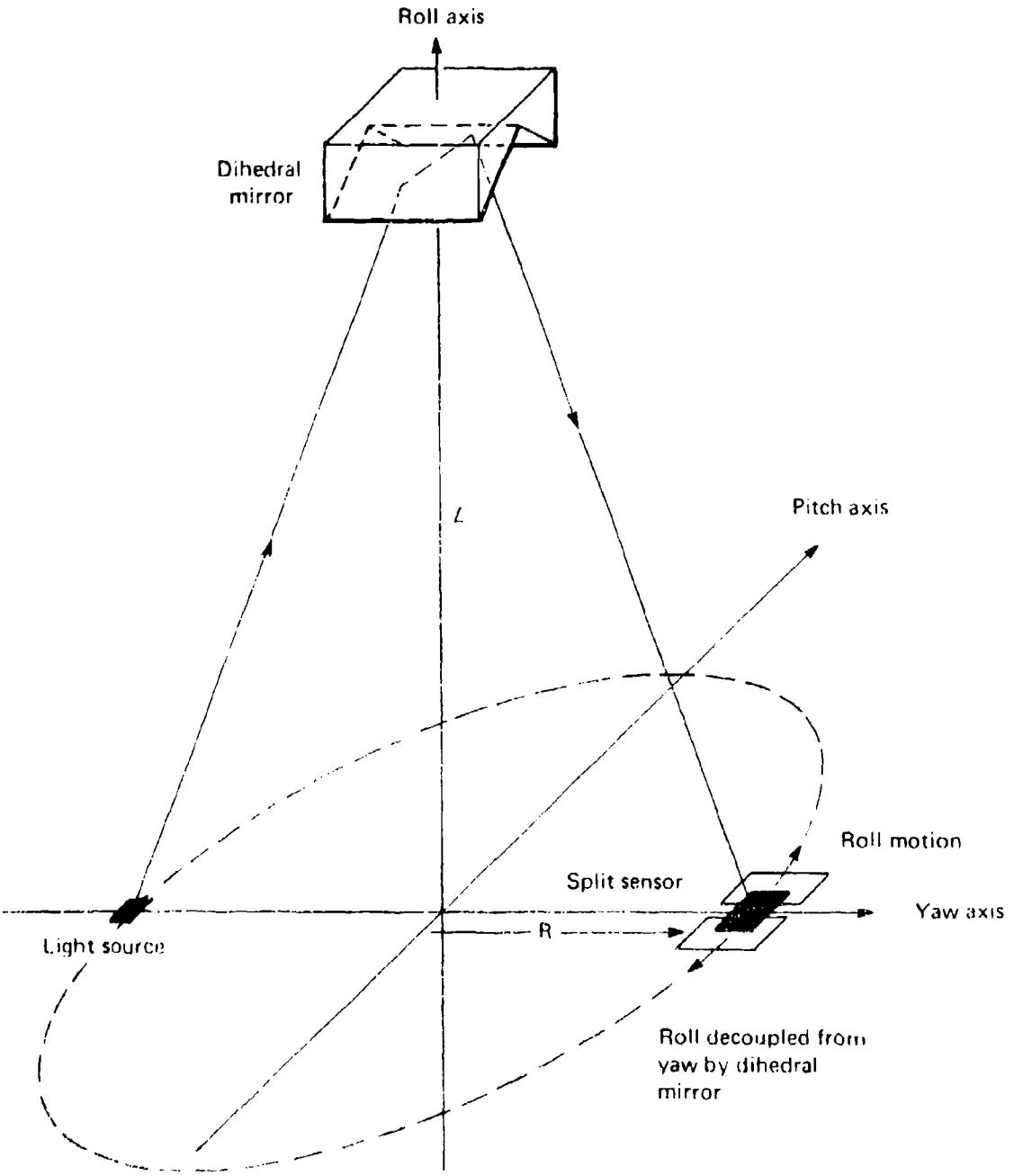


**Fig. 8 Optical Geometry for Measuring Twist**

place of calibration measurements in order to minimize the number of data channels to be telemetered.

Figure 9 is a block diagram of the two-axis pitch and yaw system, which requires four amplifier channels. The twist system is similar but requires only two amplifier channels for its single-axis measurement.

When either LED is activated, it is square-wave modulated. Each detector-amplifier channel is AC coupled, demodulated by synchronous switching, and suitably filtered. Thus an output is produced that is highly stable and exactly proportional to the square-wave light amplitude received by the detector. This output is insensitive to stray light at the detector except for the increase of shot noise.

The calibration technique consists of periodically turning on the flood LED and equally illuminating all four detectors. The outputs of channels, B, C, and D are forced equal to that of channel A by means of three separate closed loops that adjust the respective channel gains. The sample and hold circuits provide the necessary memory so that the gain correction will hold during the pitch and yaw measurements. Another loop adjusts the current into the flood beam LED to keep a constant output at channel A so that the light output of the LED is fairly constant. The flood period thus ensures that the gains of the four channels are equal.

In the measurement period, the flood beam LED is extinguished and the singal LED turned on. The square of light is focused onto the top of the pyramid (via reflection from the mirror at the magnetometer). Each of the four faces of the pyramid reflects its received light into its associated detector-amplifier channel. Deflection in the pitch direction is measured by properly combining the outputs of the four channels (A + B - C - D) as in a conventional four-quadrant detector. Similarly, yaw is obtained by combining B + D - A - C. To establish a constant scale factor, the required normalization is accomplished with another loop, which adjusts the current into the signal LED so that the sum of the four outputs remains constant.

Another method of normalization was considered. Instead of adjusting the signal LED current, the outputs are modified by dividing by the sum (A + B + C + D). With this approach, the LED output is always maximum so as to maximize the signal-to-noise ratio, but at the expense of additional circuitry.

Following the pitch and yaw output levels are A/D converters and holding registers to deliver pitch and yaw data in digital form. Ten bits will be more than adequate here; with a dynamic range of ±3 arc minutes, the resolution is 0.35 arc seconds.

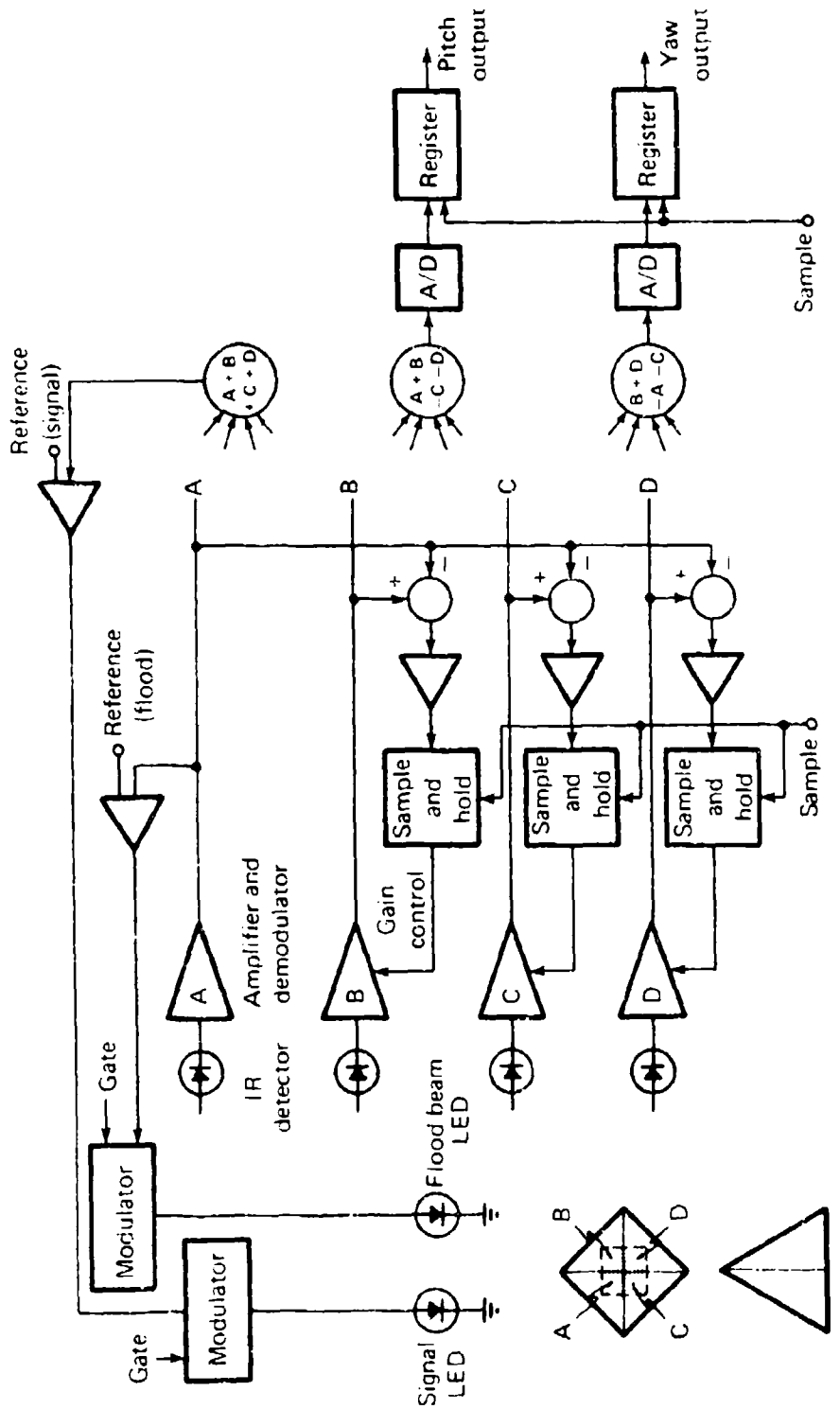


Fig. 9 Pitch/Yaw System

## MECHANICAL DESIGN

The actual mechanical design of the ATS is not included in this phase of the effort. However, the pitch/yaw and twist units of the ATS have been examined for tolerance limitations on mechanical positioning and motion of individual components. An angular positional shift or motion due to mechanical instability of the pitch/yaw package located on the instrument module or of its respective mirror on the experiment platform will result in a measured attitude translation equal to twice the actual motion. Mechanical instability of the twist package results in a more complex measurement error. The encountered instabilities are mainly thermomechanical.

The components of the pitch/yaw package (Fig. 4) whose thermomechanical stabilities are critical are the objective optic, source aperture, flat splitter, and pyramid splitter. The stability of these components must be controlled to a precision on the order of 1 arc second. The initial angular alignment of the pyramid splitter need only be performed to arc minute precision.

The components of the twist package whose thermomechanical stabilities are critical are the source aperture, transmitter projection optic, and receiver prism splitter. They also must be controlled to arc-second stability. Again, the initial alignment of the prism splitter need only be performed to arc-minute precision. Needless to say, the thermomechanical stability of the two mirrors located on the experiment platform must be in the 1-arc-second domain.

The thermomechanical stability of the twist-sensor system's receiver and transmitter packages relative to one another and to the instrument module common optical bench, which also houses the star sensor cameras, is most critical. Figure 10 illustrates four design possibilities using combinations of collimated and focused optical beams and single and double dihedral mirrors. Listed in the illustration are the permissible tolerance levels, each of which will result in a maximum error of 1 arc second in the twist measurement. It becomes apparent that either a focused or a collimated system using a single dihedral mirror offers the best stability. The detailed design stability limitations of the instrument module optical bench will affect the selection of a focused versus a collimated twist sensor. The ultimate design of the optical bench and the ATS are interdependent. (The design of the optical bench is not discussed in this report.)

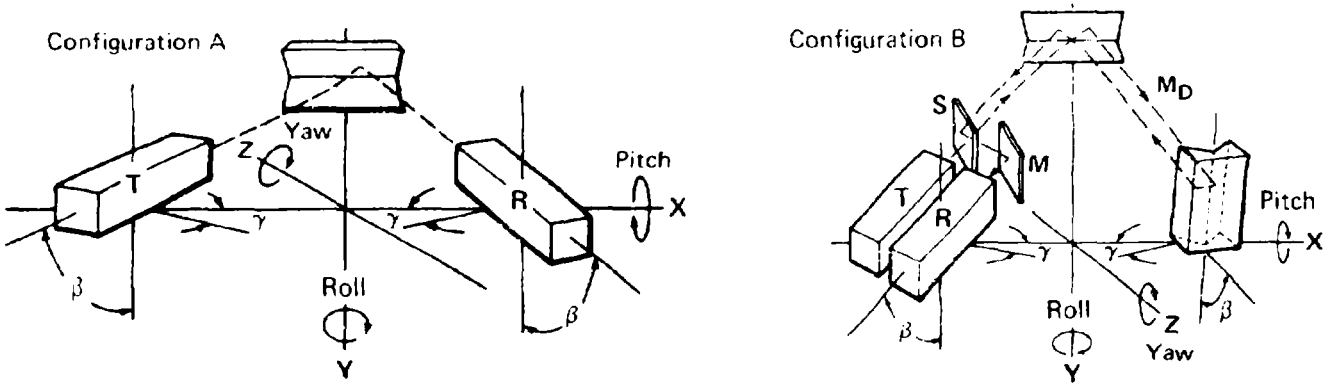


| | Focused Beam | | Collimated Beam | |
|---|---|---|---|---|
| | A | B | A | B |
| Pitch (transmitter) ± | 0.1 s | 0.05 s | 0.1 s | 0.1 s |
| Pitch (receiver) ± | 30 s | 30 s | 0.1 s | 0.1 s |
| Roll (transmitter/receiver) ± | 1 s | 10 s | 1 s | 10 s |
| Yaw (transmitter/receiver) ± | 30 s | 30 s | 20 s | 1 min |
| X (deflection) ± | 0.01 in. | 0.01 in. | 0.01 in. | 0.01 in. |
| Y (deflection) ± | 0.01 in. | 0.01 in. | 0.01 in. | 0.01 in. |
| Z (deflection) ± | 0.0001 in. | 0.01 in. | 0.01 in. | 0.01 in. |
| $\gamma$ ± | 10 s | 1 min | 10 s | 1 min |
| $\beta$ ± | 10 s | 1 min | 10 s | 1 min |
| $\alpha$ ± | 4 s | 1 min | 10 s | 1 min |
| Pitch (dihedral base M) ± | | 0.05 s | | 0.05 s |
| Roll (dihedral base M) ± | | 0.5 s | | 0.5 s |
| Yaw (dihedral base M) ± | | insensitive | | insensitive |
| Twist sensitivity* | 1 | 1 | 0.05 | 0.05 |

*Relative to focused beam, configuration A

**Fig. 10 Twist Sensor System Tolerances for Arc-Second Accuracy**

# 4. SYSTEM INTEGRATION AND TESTING

The attitude-determination system requires highly precise interalignment of its various subsystems, i.e., star sensor cameras, ATS, solar attitude sensor, and vector magnetometer experiment package. It is essential that each of these subsystems be precisely aligned with an accessible reference surface or mirror. The ATS and the star sensor cameras must allow alignment relative to one another and to their common optical bench when measured both independently and integrated with the satellite.

In order to assure proper operation and accuracy of the star sensors and the ATS in a "zero g" flight environment, it is necessary to make total system optical alignment measurements in the normal flight position and when rotated 180°. If under both conditions the systems maintain alignment within the required specifications, then the proper alignment at zero g is assured. The arrangement shown in Fig. 11 permits alignment and alignment measurement of the optical bench and its optical systems as a separate unit or when integrated with the satellite.

In this approach, a common collimated star source is generated at star sensor, SS, and split by mirrors on precision angular rotaries to enter the star cameras at the desired angle via $M_3$ and $M_4$. The star source, also used as an autocollimator, is autocollimated with mirrors $M_1$ and $M_2$ by means of a precision rotary prism/mirror system, P and $M_3$. The ATS is also autocollimated against mirrors $M_1$ and $M_2$, thereby providing a common reference for measurements of the boresight angles between the star cameras and the ATS. When making alignment measurements of the total system in the inverted position, mirrors $M_5$, $M_6$, $M_7$, $M_8$, and $M_1$ are used. The entire mirror complex must be aligned to arc-second precision. It is mounted on a precision rotary base and a theodolite is used to perform the alignment.

The fixturing, P, mounted to the precision two-axis gimbal is only for initial alighment. The optical bench, either separately or integrated with the satellite, is mounted to this large precision gimbal (Fig. 12). When the optical bench is being aligned and tested as a separate unit, mirrors $M_1$ and $M_2$ are used instead of the mirror fixed to the magnetometer. When the whole satellite is being alignment tested, the experiment package at the end of the boom is rested on a precision positioning head affixed to the same support pedestal as is the mirror, $M_1$ or $M_2$. The change in virtual boom length when using mirror $M_1$ or $M_2$ (on the

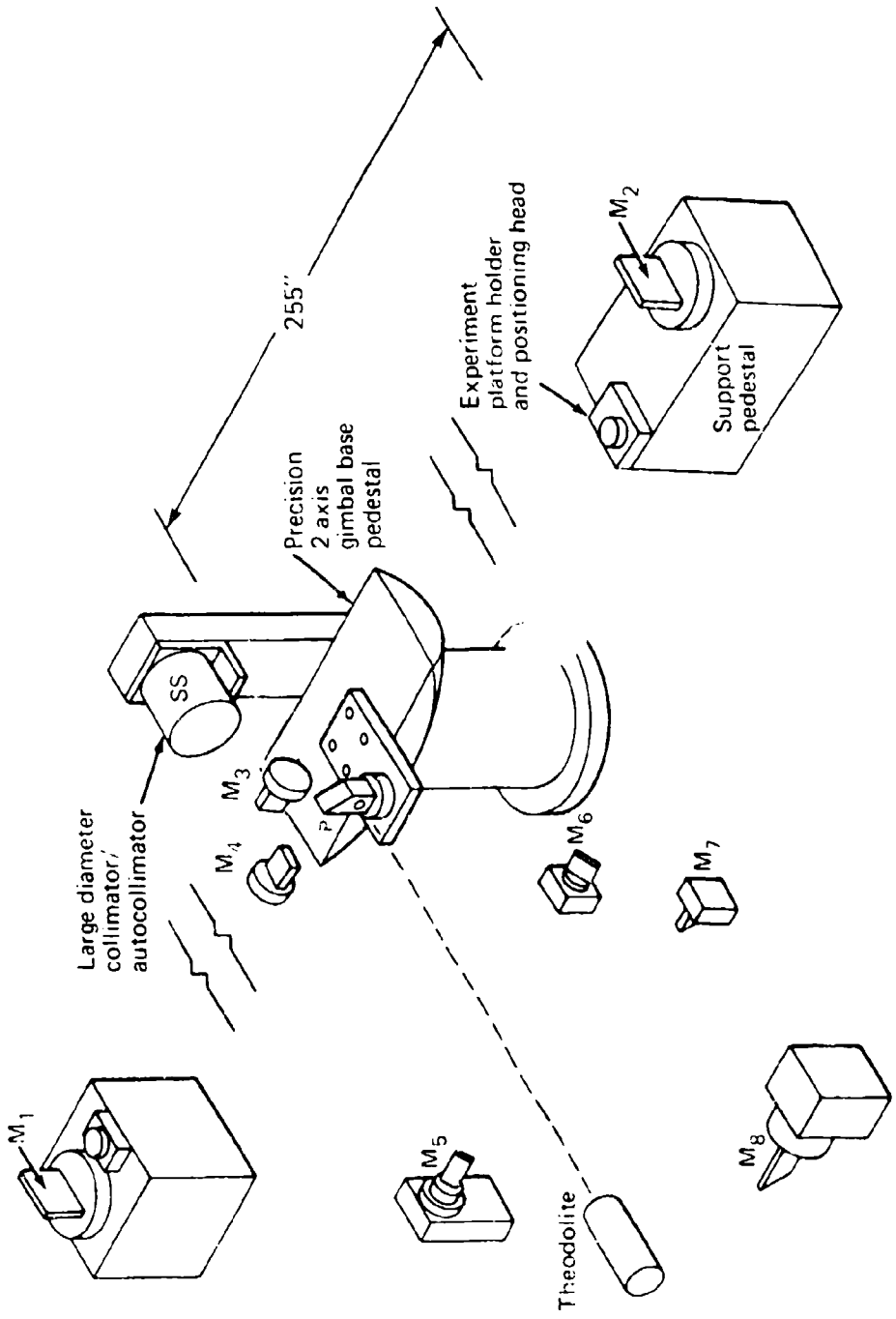


**Fig. 11 Optical Metrology Instrumentation**

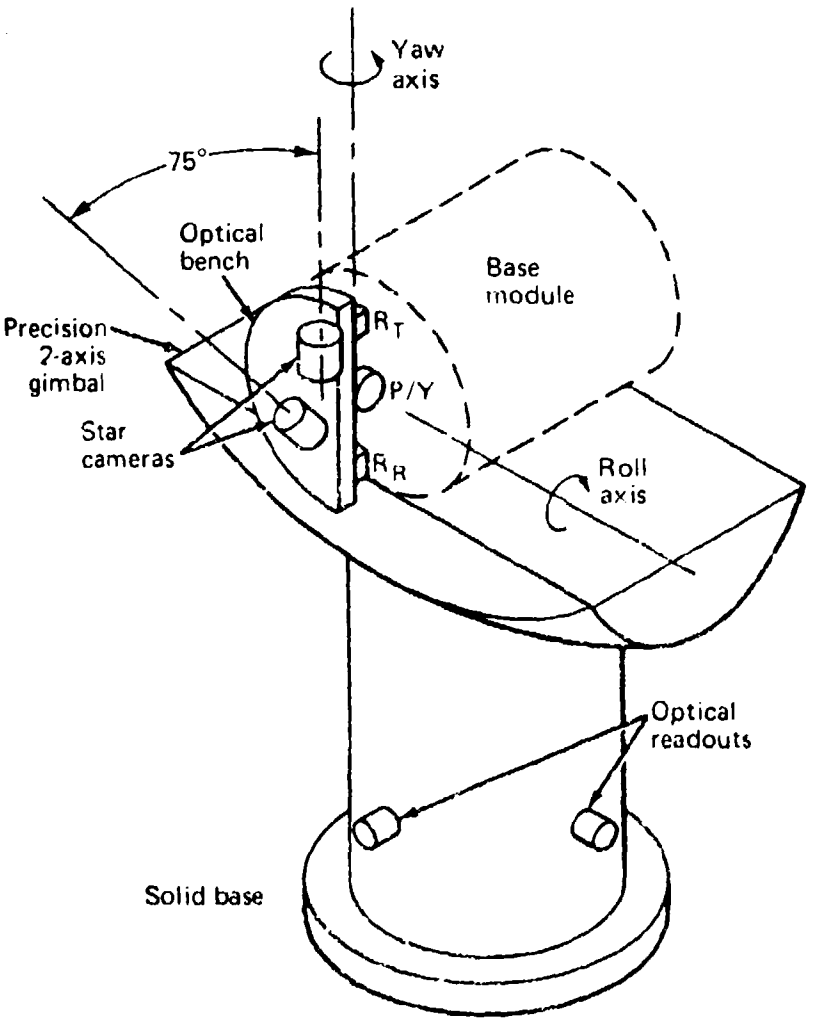


Fig. 12 Satellite and Optical Systems on Base Pedestal

order of 15 in.) results in an optical offset in the twist sensor. This offset is of no major consequence for a collimated twist system, but it must be taken into account in a focused system.

An alternate approach to total system alignment is one in which the star cameras and the ATS are not activated and cannot be aligned in a single setup. The alignment instrumentation, however, is contained in one setup as shown in Fig. 13. (The system is somewhat simpler to implement than that shown in Fig. 11.) It may be observed in Fig. 13 that diametrically opposed mirror and collimation systems are used to perform inversion alignments and thereby negate g loading effects (unit 1: $A_1$, $M_1$, $M_2$, $M_3$, $R_4$; unit 2: $M_8$, $M_9$, $M_{10}$, $A_3$, $R_3$). The mirrors, $M_4$ and $M_5$, and the precision rotary table, $R_4$, located on the precision two-gimbal mount, $R_2$, are for autocollimation of the total mirror system by means of the autocollimator, $A_2$, and its mirrors, $M_6$ and $M_7$. The objective is to autocollimate and establish orthogonality between $A_1$, $A_2$, and $A_3$ with their dual-beam outputs and mirrors $M_3$ and $M_{10}$.

Figure 14 shows the configuration with the satellite (or optical bench) for ATS alignment measurement. The optical bench is equipped with a precision measurement prism, P, that has been separately autocollimated against the reference mirror on star sensor, $SS_2$. The optical bench is properly oriented on the two-axis gimbal, $R_2$, via autocollimation techniques with respect to two orthogonal surfaces on prism, P, using autocollimator, $A_2$. Since $M_{10}$ has already been collimated against $A_2$ (see Fig. 13), it is possible to activate the pitch/yaw sensor of the ATS for alignment measurement against $M_{10}$. The pitch/yaw boresight axis is established against prism P, which is used as a reference for all alignment measurements. Affixed to the mirror mount, $M_{10}$, is a vertical dihedral mirror in addition to the autocollimation flat. The vertical roof line of the dihedral mirror has been previously sighted and aligned by means of the autocollimation telescope, $A_2$. The twist (roll) portion of the ATS is aligned against the dihedral mirror. The experiment platform, which carries the flight flat and dihedral mirrors, is fastened to a small two-axis positionable gimbal, $R_3$. The ATS is now activated against the mirror system as a check on the positioning precision of the extendable boom and on the angular control range. This procedure is repeated with the satellite optical bench rotated 180° using the complementary setup on alignment pad No. 2.

The satellite optical bench is now rotated to the position shown in Fig. 15. Here the satellite optical bench is precisely oriented by autocollimation using $A_2$ against two orthogonal faces of the precision prism, P. The collimator, $A_1$, is turned on to produce a point image in the star sensor, $SS_2$. This image location is read out of the star sensor relative to its electrical

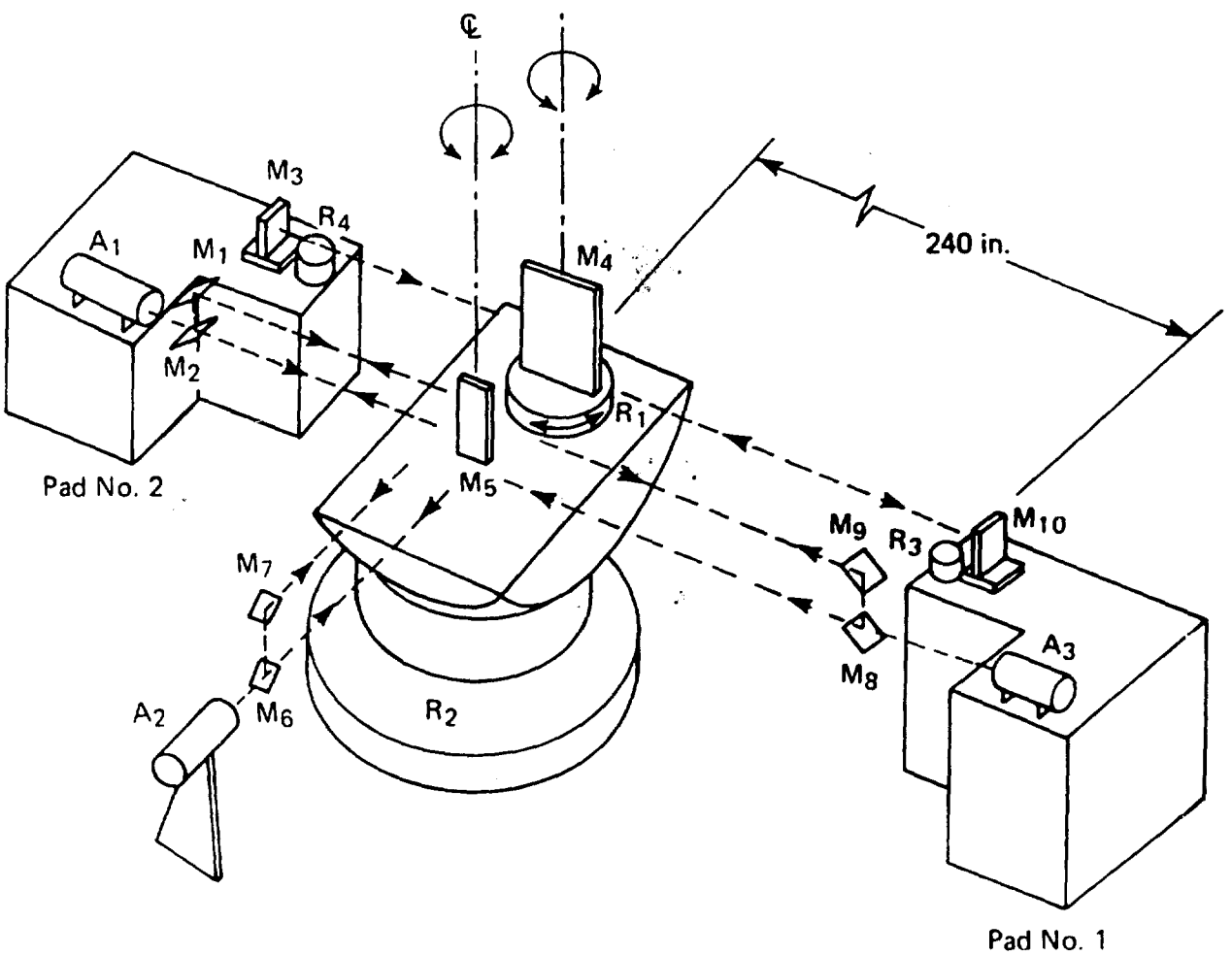


Fig. 13 Gen[illegible]ment Configuration of Optical Test Stand

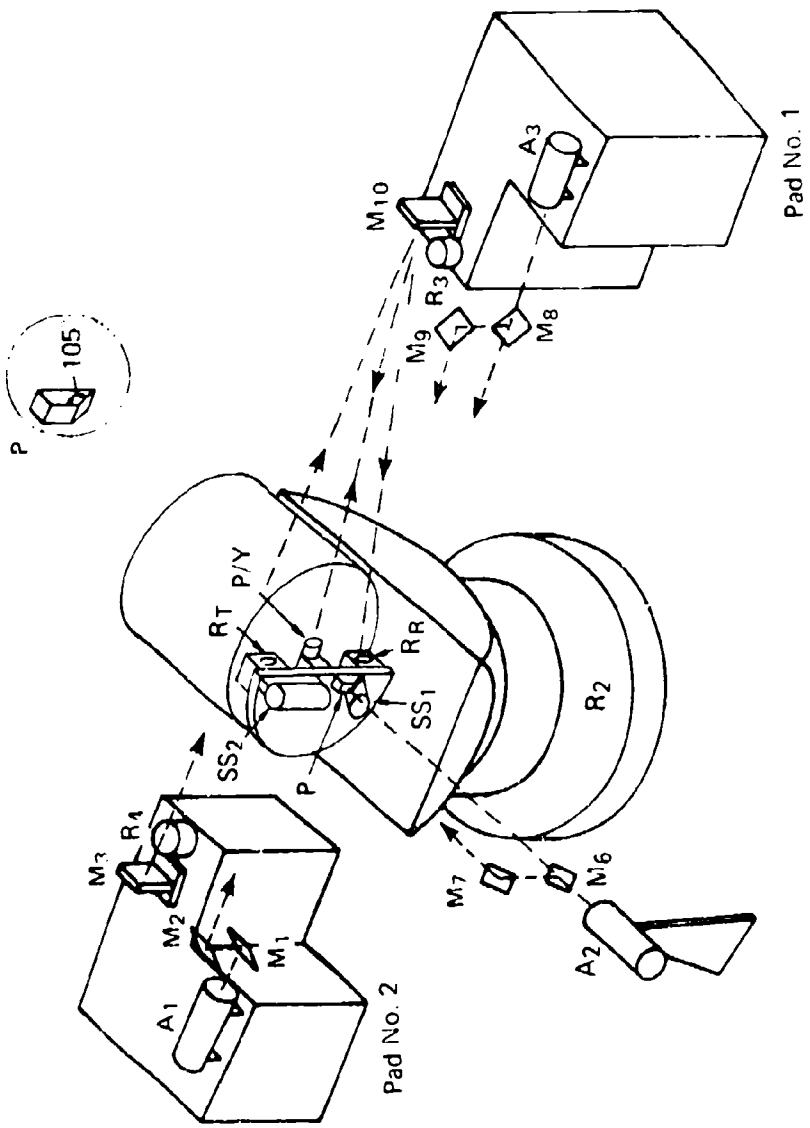


Fig. 14 Optical Setup for ATS/Satellite Optical Bench Alignment

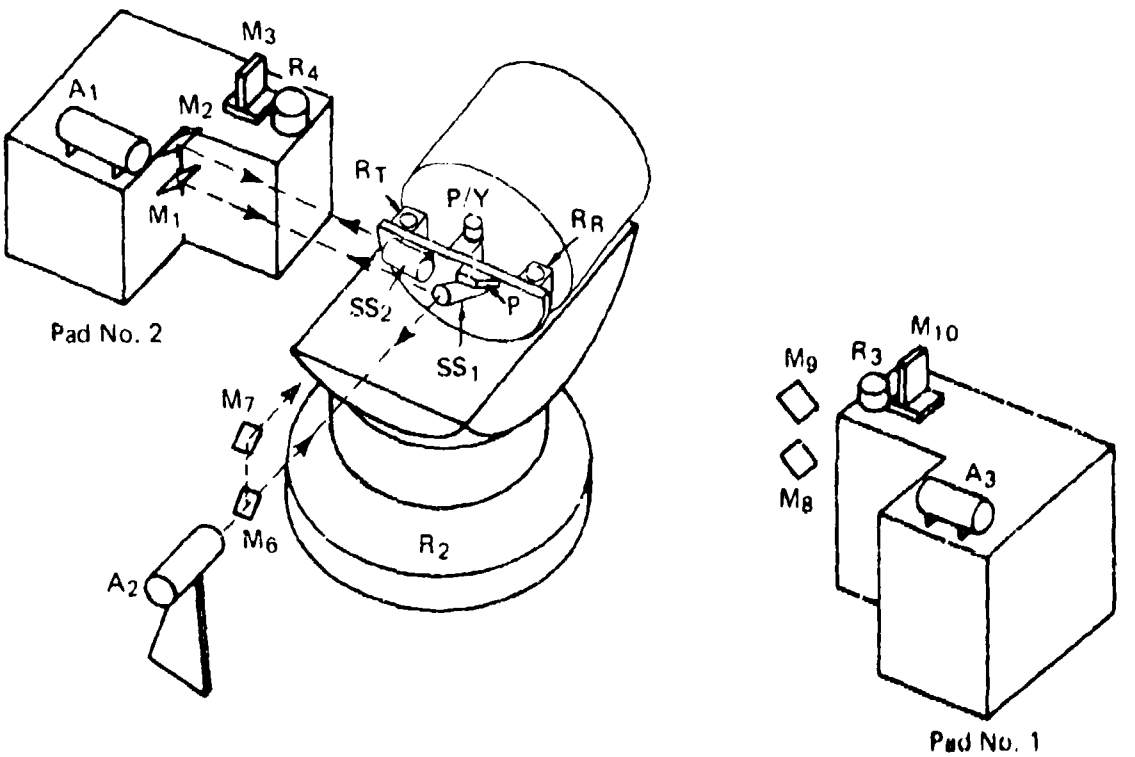


**Fig. 15 Optical Setup for Star Sensor/Satellite Optical Bench Alignment**

boresight, which in turn is computed relative to the prism, P. The optical bench (satellite) is now rotated a precise 75° as determined by autocollimation against the 105° face on prism, P, using $A_2$. A collimated optical beam is now fed into star sensor $SS_1$ via $A_1$ and $M_1$ (which is a splitter). The coordinate readout of the point image produced in $SS_2$ is compared to the $SS_2$ electrical boresight and the prism, P. This procedure is repeated with a 180° system rotation to nullify g loading.

The optical axes of the two star sensors are now known relative to the prism, P, and the ATS coordinate axes are also known relative to P; therefore, the star sensors and the ATS coordinate axes are known relative to one another.

The solar attitude detector (which is mounted to the experiment package) is aligned against the vector magnetometer reference mirror and the ATS flat mirror by means of theodolite autocollimation.

The details of the procedures for the optical alignment measurements are far more extensive than is indicated in this report. They will be the subject of a subsequent phase of the program.

## Appendix A

### SIGNAL-TO-NOISE COMPUTATIONS FOR PITCH/YAW/TWIST

The significant computation to be made for any of the attitude transfer axes is

$$\frac{\text{Differential signal}}{\text{Noise}} ,$$

where the differential signal corresponds to the angular resolution capability of the particular system.

PITCH/YAW SYSTEM

The desired ratio is

$$\Delta S_{p/y}/i_N ,$$

where

$\Delta S_{p/y}$ = incremental signal change at the detector output, and

$i_N$ = combined noise.

To compute $\Delta S_{p/y}$ it is essential to take into consideration the system optical components and their transmission factors.

Progression of Optical Efficiency per Channel

Transmitter

| | |
|---|---|
| Light-pipe/condenser | $\beta_1 = 0.2$ |
| Aperture | $\beta_2 = 0.8$ |
| Splitter (flat) | $\beta_3 = 0.5$ |
| Projection objective | $\beta_4 = 0.85$ |
| Filter | $\beta_5 = 0.90$ |
| Mirror (at experiment) | $\beta_6 = 0.9$ |

Receiver

| | |
|---|---|
| Filter | $\beta_5 = 0.9$ |
| Objective optic | $\beta_4 = 0.85$ |
| Splitter | $\beta_3 = 0.5$ |
| Pyramid splitter | $\beta_7 = 0.25$ |
| Pyramid splitter reflection | $\beta_8 = 0.9$ |
| Condenser optic | $\beta_9 = 0.8$ |

Combined optical efficiency,

$$E = \beta_1 \beta_2 \beta_3^2 \beta_4^2 \beta_5^2 \beta_6 \beta_7 \beta_8 \beta_9$$

$$= 3.79 \times 10^{-3} \quad .$$

The electrical signal level at the output of any individual channel for a boresight condition may be expressed as

$$S_{P/\gamma} = PE\gamma \quad ,$$

where

S = output current at detector (A),

P = source power output (W), and

$\gamma$ = detector sensitivity (A/W).

For an RCA SG-1009 IR LED source,

$P = 10^{-3}$ W peak with derating at 1 kHz PRF.

For an HP-5082-4207 silicon diode detector,

$\gamma = 0.65$ A/W.

For $E = 3.79 \times 10^{-3}$ (see tabulation),

$$S_{P/\gamma} = 10^{-3} (3.79)10^{-3} (0.65) = 2.46 \times 10^{-6} \text{ A}.$$

The change in signal level due to an incremental pitch or yaw change of 1 arc second is given as 1 part in 180 (see Fig. 6). Therefore

$$\Delta S_{P/Y} = \frac{S_{P/Y}}{180} = \frac{2.46 \times 10^{-6}}{180} = 1.36 \times 10^{-8} \text{ A.}$$

The noise in any channel of the pitch/yaw system is a combination of shot noise, detector generation-recombination noise, and Johnson noise at the preamplifier.

Shot Noise (SN)

$$\bar{i}_{SN} = \sqrt{2ei_s(\Delta F)} \ ,$$

where

$\bar{i}_{SN}$ = rms noise current,

$e$ = electronic charge = $1.6 \times 10^{-19}$ C,

$i_s$ = signal current, and

$\Delta F$ = system bandwidth at detector.

If $i_s = P_{S/Y}$ and $\Delta F = 2 \times 10^3$ Hz,* then

$$\bar{i}_{SN} = \sqrt{(2)(1.6)10^{-19} \ (2.46)10^{-6} \ (2)10^3}$$

$$= 1.57 \times 10^{-21} \ .$$

Generation-Recombination Noise (GR)

This noise is given as detector noise equivalent power (NEP) in $W/Hz^{\frac{1}{2}}$. The detector specifications list NEP as $3.6 \times 10^{-14}$ $W/Hz^{\frac{1}{2}}$. For a 2-kHz bandwidth,

$$i_{GR_N} = (3.6)10^{-14} \ (2 \times 10^3)^{\frac{1}{2}}$$

$$= 1.6 \times 10^{-12} \text{ A.}$$

*The actual processing bandwidth of the modulated signal may be on the order of a few hertz.

Johnson Noise (JN)

$$i_{JN} = \left[\frac{4KT(\Delta F)}{R}\right]^{\frac{1}{2}},$$

where

K = Boltzmann's constant = $1.38 \times 10^{-23}$ W-s/deg,

T = absolute temperature = 300°K,

R = noise resistance = $5 \times 10^{6}$ Ω, and

$\Delta F$ = bandwidth = $2 \times 10^{3}$ Hz.

Therefore

$$i_{JN} = \left[\frac{(4)(1.38)10^{-23}\ (2)10^{3}}{(5)10^{6}}\right]^{\frac{1}{2}} = 1.48 \times 10^{-13}\ \text{A}.$$

The combined noise at the detector output is

$$i_N = (i_{SN}^{\ 2} + i_{GR_N}^{\ 2} + i_{JN}^{\ 2})^{\frac{1}{2}}$$

$$= 1.6 \times 10^{-12}\ \text{A}.$$

The noise voltage ($V_N$) is the product of $i_N$ and R, the load resistance:

$$V_N = (1.6)10^{-12}\ (5)10^{6} = 8 \times 10^{-6}\ \text{V}.$$

The noise contribution of an LM108 preamplifier is quoted as

$$v_n = 0.5 \times 10^{-6}/\text{Hz}^{\frac{1}{2}}.$$

For $\Delta F = 2 \times 10^{3}$ Hz,

$$v_n = \frac{5 \times 10^{-7}}{\left[(2)10^{3}\right]^{\frac{1}{2}}} = 1.11 \times 10^{-8}\ \text{V}.$$

The amplifier noise is negligible in comparison to the other sources.

The value of $\Delta S_{P/Y}/i_N$ can now be computed:

$$\frac{\Delta S_{P/Y}}{i_N} = \frac{1.36 \times 10^{-8}}{1.6 \times 10^{-12}} = 8.54 \times 10^{3} \text{ (for 1 arc second)}$$

$$= 78 \text{ dB}$$

if viewed as a voltage ratio at the output of the LM108 preamplifier or if viewed as a current ratio at the detector output.

TWIST SYSTEM

The computation for the twist system is identical to that for the pitch/yaw system with the exception of the optical efficiency, E, and the incremental signal change per angular resolution element of 1 part in 602 per detector (collimated system) for 5 arc seconds (see Fig. C-1 in Appendix C). For a focused or collimated system, the value of E is computed from the following tabulation.

Prognosis of Optical Efficiency per Channel

| | |
|---|---|
| Transmitter | |
| Light-pipe/condenser | $\beta_1 = 0.2$ |
| Aperture | $\beta_2 = 0.8$ |
| Projection optic | $\beta_3 = 0.85$ |
| Filter | $\beta_4 = 0.90$ |
| Dihedral mirror (two bounces) | $\beta_5 = 0.81$ |
| Receiver | |
| Filter | $\beta_4 = 0.90$ |
| Prism splitter | $\beta_5 = 0.50$ |
| Prism splitter reflection | $\beta_6 = 0.90$ |
| Condenser optic | $\beta_7 = 0.80$ |
| Objective optic (collimated system only) | $\beta_8 = 0.85$ |

Combined optical efficiency,

$$E = \beta_1 \beta_2 \beta_3 \beta_4^2 \beta_5^2 \beta_6 \beta_7$$

$$= 3.2 \times 10^{-2} \text{ (focused system)}$$

or

$$= 2.7 \times 10^{-2} \text{ (collimated system).}$$

$$\Delta S_R = \frac{PE\gamma}{602} = \frac{10^{-3} (2.7)10^{-2} (0.65)}{602}$$

$$= 2.92 \times 10^{-8} \text{ A.}$$

$$\frac{\Delta S_R}{i_N} = \frac{2.92 \times 10^{-8}}{1.6 \times 10^{-12}} = 1.8 \times 10^4 \text{ (for 5 arc seconds)}$$

$$= 85 \text{ dB.}$$

Again, as in the pitch/yaw system, there is an adequate differential signal-to-noise ratio.

## Appendix B

## MEASUREMENT OF TWIST BY MEANS OF A DIHEDRAL MIRROR

The twist angle of a distant object may be measured by aiming a collimated beam at a tilted mirror mounted on the object and measuring the angle of the reflected beam. In the case illustrated in Fig. 2, where the incident and reflected beams are in a vertical plane, twist is measured by the change in horizontal angle of the reflected beam. However, the horizontal angle is also affected, and to a much greater degree, by the yaw of the mirror. It is well known that the substitution of a Porro prism (or its equivalent, a dihedral mirror) aligned with the yaw axis makes the reflected beam insensitive to yaw. It is the purpose of the ensuing exercise to demonstrate that the cross-coupling effects resulting from confining yaw with a small amount of roll (twist) are all higher order. Thus a measurement of the horizontal angle of the reflected beam yields twist information and is essentially independent of yaw. The analysis determines the direction cosines X′,Y′,Z′ of the first ray after an incoming ray with direction cosines X,Y,Z is doubly reflected by the dihedral mirror.

The mirrors form a right angle along the y axis and are yawed at an angle θ about the y axis (see sketch). The direction cosines of the normal to mirror 1 are

$$L_1 = \cos\theta, \quad M_1 = 0, \quad N_1 = -\sin\theta.$$

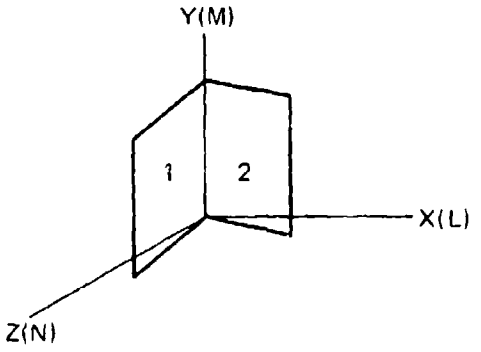


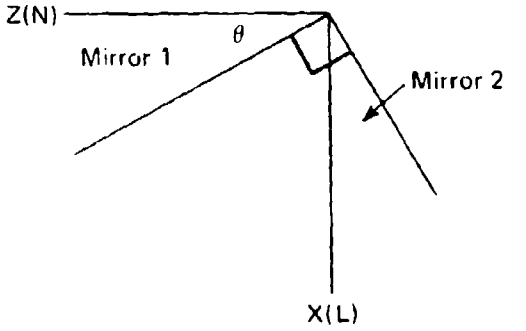

The direction cosines of the normal to mirror 2 are

$$L_2 = \sin\theta, \quad M_2 = 0, \quad N_2 = \cos\theta.$$

Now let the mirrors roll a small angle $\phi$ about the x axis. This is equivalent to rolling the coordinate axes about the x axis in the opposite direction. We may find the new mirror normals using the rotation matrix:

| | x | y | z |
|---|---|---|---|
| x′ | 1 | 0 | 0 |
| y′ | 0 | cos $\phi$ | -sin $\phi$ |
| z′ | 0 | sin $\phi$ | cos $\phi$ |

Mirror 1

$$\begin{pmatrix} L_1' \\ M_1' \\ N_1' \end{pmatrix} = \begin{pmatrix} 1 & 0 & 0 \\ 0 & \cos\phi & -\sin\phi \\ 0 & \sin\phi & \cos\phi \end{pmatrix} \begin{pmatrix} L_1 \\ M_1 \\ N_1 \end{pmatrix}$$

$$L_1' = L_1 = \cos\theta$$

$$M_1' = M_1 \cos\phi - N_1 \sin\phi = \sin\theta \sin\phi$$

$$N_1' = M_1 \sin\phi + N_1 \cos\phi = -\sin\theta \cos\phi$$

Mirror 2

$$\begin{pmatrix} L_2' \\ M_2' \\ N_2' \end{pmatrix} = \begin{pmatrix} 1 & 0 & 0 \\ 0 & \cos\phi & -\sin\phi \\ 0 & \sin\phi & \cos\phi \end{pmatrix} \begin{pmatrix} L_2 \\ M_2 \\ N_2 \end{pmatrix}$$

$$L_2' = \sin\theta$$

$$M_2' = -\cos\theta \sin\phi$$

$$N_2' = \cos\theta \cos\phi$$

The reflection matrix is given by:

$$\begin{pmatrix} 1 - 2L^2 & -2LM & -2LN \\ -2LM & 1 - 2M^2 & -2MN \\ -2LN & -2MN & 1 - 2N^2 \end{pmatrix}$$

$$r_1 = \begin{pmatrix} 1 - 2\cos^2\theta & -2\sin\theta\cos\theta\sin\phi & 2\sin\theta\cos\theta\cos\phi \\ -2\sin\theta\cos\theta\sin\phi & 1 - 2\sin^2\theta\sin^2\phi & 2\sin^2\theta\sin\phi\cos\phi \\ 2\sin\theta\cos\theta\cos\phi & 2\sin^2\theta\sin\phi\cos\phi & 1 - 2\sin^2\theta\cos^2\phi \end{pmatrix}$$

$$= \begin{pmatrix} -\cos 2\theta & -\sin 2\theta\sin\phi & \sin 2\theta\cos\phi \\ -\sin 2\theta\sin\phi & 1 - 2\sin^2\theta\sin^2\phi & \sin^2\theta\sin 2\phi \\ \sin 2\theta\cos\phi & \sin^2\theta\sin 2\phi & 1 - 2\sin^2\theta\cos^2\phi \end{pmatrix}$$

$$r_2 = \begin{pmatrix} 1 - 2\sin^2\theta & 2\sin\theta\cos\theta\sin\phi & -2\sin\theta\cos\theta\cos\phi \\ 2\sin\theta\cos\theta\sin\phi & 1 - 2\cos^2\theta\sin^2\phi & 2\cos^2\theta\sin\phi\cos\phi \\ -2\sin\theta\cos\theta\cos\phi & 2\cos^2\theta\sin\phi\cos\phi & 1 - 2\cos^2\theta\cos^2\phi \end{pmatrix}$$

$$= \begin{pmatrix} \cos 2\theta & \sin 2\theta\sin\phi & -\sin 2\theta\cos\phi \\ \sin 2\theta\sin\phi & 1 - 2\cos^2\theta\sin^2\phi & \cos^2\theta\sin 2\phi \\ -\sin 2\theta\cos\phi & \cos^2\theta\sin 2\phi & 1 - 2\cos^2\theta\cos 2\phi \end{pmatrix}$$

For small values of $\phi$, $\cos\phi \approx 1$ and $\sin\phi = \phi$

$$r_1 = \begin{pmatrix} -\cos 2\theta & -\phi\sin 2\theta & \sin 2\theta \\ -\phi\sin 2\theta & 1 - 2\phi^2\sin^2\theta & 2\phi\sin^2\theta \\ \sin 2\theta & 2\phi\sin^2\theta & \cos 2\theta \end{pmatrix}$$

$$r_2 = \begin{pmatrix} \cos 2\theta & \phi \sin 2\theta & -\sin 2\theta \\ \phi \sin 2\theta & 1 - 2\phi^2 \cos^2\theta & 2\phi \cos^2\theta \\ -\sin 2\theta & 2\phi \cos^2\theta & -\cos 2\theta \end{pmatrix}$$

If an incoming ray of light has direction cosines X,Y,Z, then after double reflection,

$$\begin{pmatrix} X' \\ Y' \\ Z' \end{pmatrix} = \begin{pmatrix} r_2 \end{pmatrix} \begin{pmatrix} r_1 \end{pmatrix} \begin{pmatrix} X \\ Y \\ Z \end{pmatrix}$$

Z′ will be a measure of twist angle $\phi$:

$$Z' = A_{31} X + A_{32} Y + A_{33} Z$$

$$A_{31} = \sin 2\theta \cos 2\theta - 2\phi^2 \sin 2\theta \cos^2 \theta - \sin 2\theta \cos 2\theta$$
$$= -2\phi^2 \sin 2\theta \cos^2 \theta$$

$$A_{32} = \phi \sin^2 2\theta + 2\phi \cos^2 \theta (1 - 2\phi^2 \sin^2 \theta) - 2\phi \sin^2 \theta \cos 2\theta$$

$$A_{33} = -\sin^2 2\theta + 4\phi^2 \sin^2 \theta \cos^2 \theta - \cos^2 2\theta$$
$$= -1 + 4\phi^2 \sin^2 \theta \cos^2 \theta$$

Neglecting higher-order terms,

$$A_{31} = 0$$

$$A_{32} = \phi(\sin^2 2\theta + 2 \cos^2 \theta - 2 \sin^2 \theta \cos^2 \theta)$$
$$= \phi(\sin^2 2\theta + 1 + \cos 2\theta - 2 \sin^2 \theta \cos 2\theta)$$
$$= \phi(\sin^2 2\theta + 1 + \cos 2\theta [1 - 2 \sin^2 \theta])$$
$$= \phi(\sin^2 2\theta + 1 + \cos^2 2\theta)$$
$$= 2\phi$$

$$A_{33} = -1$$

Therefore

$$Z' = 2\phi Y - Z$$

and is independent of $\theta$.

Other components of the reflected ray are:

$$X' = A_{11} X + A_{12} Y + A_{13} Z$$

$$A_{11} = -\cos^2 2\theta - \phi^2 \sin^2 2\theta - \sin^2 2\theta$$
$$\approx -1$$

$$A_{12} = -\phi \sin 2\theta \cos 2\theta + \phi \sin 2\theta (1 - 2\phi^2 \sin^2 \theta)$$
$$-2\phi \sin^2 \theta \sin 2\theta$$
$$\approx -\phi(\sin 2\theta \cos 2\theta - \sin 2\theta + 2 \sin^2 \theta \sin 2\theta)$$
$$= -\phi \sin 2\theta (\cos 2\theta - 1 + 2 \sin^2 \theta)$$
$$= 0$$

$$A_{13} = \sin 2\theta \cos 2\theta + 2\phi^2 \sin^2 \theta \sin 2\theta - \sin 2\theta \cos 2\theta$$
$$\approx 0$$

Therefore

$$X' = -X.$$

$$Y' = A_{21} X + A_{22} Y + A_{23} Z$$

$$A_{21} = -\phi \sin 2\theta \cos 2\theta - \phi \sin 2\theta (1 - 2\phi^2 \cos^2 \theta)$$
$$+2\phi \sin 2\theta \cos^2 \theta$$
$$\approx -\phi \sin 2\theta (\cos 2\theta + 1 - 2 \cos^2 \theta)$$
$$= 0$$

$$A_{22} = -\phi^2 \sin^2 2\theta + (1 - 2\phi^2 \cos^2\theta)(1 - 2\phi^2 \sin^2 \theta) + 4\phi^2 \sin^2 \theta \cos^2 \theta$$

$$\approx 1$$

$$A_{23} = \phi \sin^2 2\theta + 2\phi \sin^2\theta \ (1 - 2\phi^2 \cos^2 \theta) + 2\phi \cos^2 \theta \cos 2\theta$$

$$= \phi \ (\sin^2 2\theta + 2 \sin^2 \theta + [1 + \cos 2\theta] \cos 2\theta)$$

$$= \phi \ (\sin^2 2\theta + 2 \sin^2 \theta + \cos^2 2\theta + \cos 2\theta)$$

$$= \phi \ (1 + 2 \sin^2 \theta + 1 - 2 \sin^2 \theta)$$

$$= 2\phi$$

**Therefore**

$$Y' = Y + 2\phi Z.$$

If the original ray is vertical, $Z = 0$ and $Y' = Y$. If the original ray is not vertical, there is a $Y$ displacement with twist (immaterial to measurement since we are measuring $Z$ and pitch will produce a much greater motion of $Y'$).

# Appendix C

## GEOMETRIC/OPTICAL CONSIDERATIONS OF A TWIST SENSOR

### COLLIMATED SYSTEM

The geometry of a collimated beam twist sensor is complex (see Fig. C-1). Basically, the change in position of the transmitted optical image in the receiver objective optic image plane is indicative of twist in the dihedral mirror that is fastened to the magnetometer experiment. The sensitivity to the position of the image square, which is split across the roof line of the receiver reflective prism, depends on the beam length, L; the transmitter/receiver base circle radius, R; the focal length, FL, of the receiver optic; and the linear dimension of the image square. The sample calculation in Fig. C-1 is typical. A twist of 5 arc seconds results in a differential receiver signal change of 1 part in 300, which is easily detectable. It must be remembered that twist appears at the receiver as a pseudo-yaw motion. Any pitch motion in the system is in the orthogonal direction or along the roof line of the receiver mirrored prism splitter (Fig. 7). Therefore the prism must be long enough to accommodate a pitch motion of at least ±3 arc minutes. This can be equated to a linear motion along the prism roof line as follows:

$$p = \pm P(FL)$$

where

$p$ = linear pitch motion in the image plane,

$\pm P$ = tolerable pitch angular motion, and

$FL$ = focal length of receiver objective optic.

If

$$P = \pm 3 \text{ arc minutes} = 8.72 \times 10^{-4} \text{ rad},$$

and

$$FL = 8 \text{ in.},$$

then

$$p = \pm 6.98 \times 10^{-3} \text{ in.}$$

It is apparent that the prism can be small, i.e., the optical image size plus 2p as a minimum. For an optical image of 0.028 in., a prism larger than 0.042 $in^2$ is required. This is also the minimum requirement for the diameter of the condenser optic.

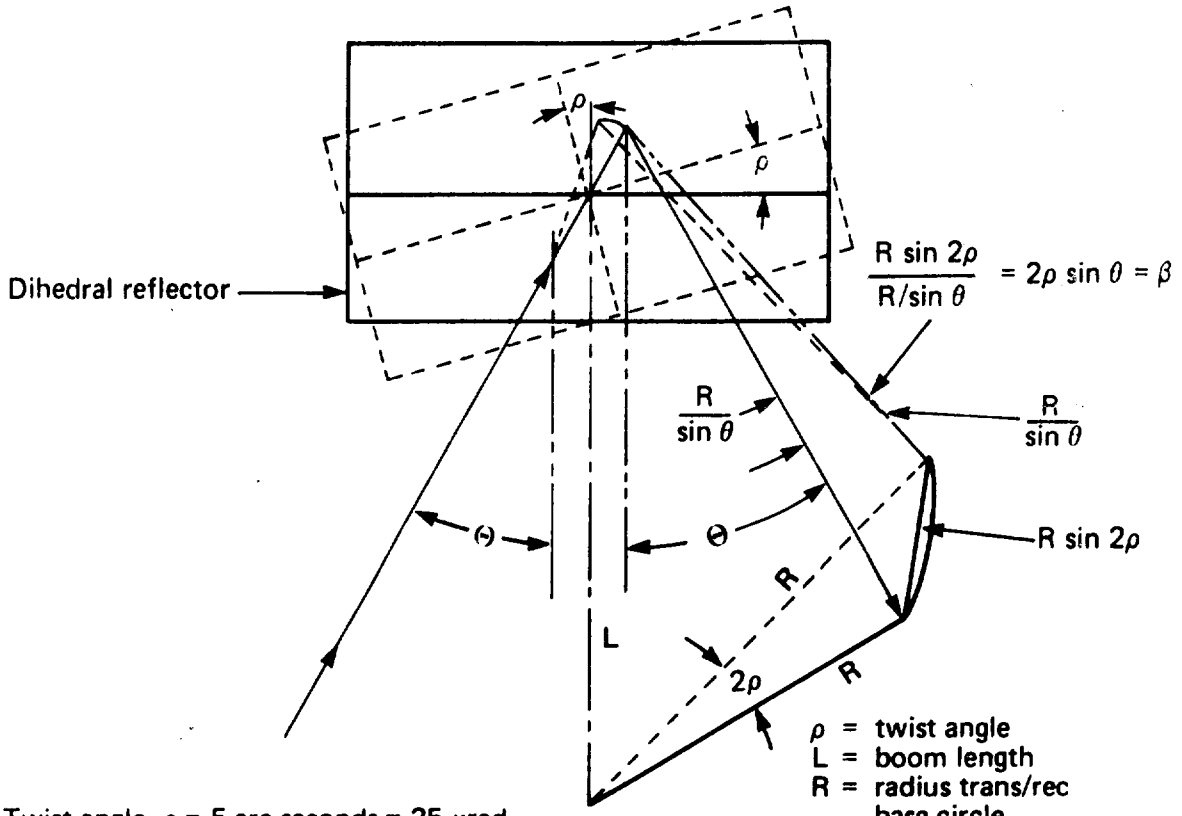


ρ = twist angle
L = boom length
R = radius trans/rec base circle
θ = angle of incidence or reflected ray with nulled axis of symmetry
FL = focal length of receiver optic

Twist angle, $\rho$ = 5 arc seconds = 25 μrad
Image plane displacement (pseudo-yaw):
$y = \beta (FL) = (2\rho \sin \theta)\, FL$ where FL = 8 in.

$$\theta = \sin \theta = \tan \theta = \frac{R}{L} = \frac{10}{240} = \frac{1}{24}$$

$y = 1.66 \times 10^{-5}$ in.
Signal incremental change for 5 arc seconds (2 detector elements):

$$\Delta = \frac{2yl}{l^2} = \frac{(2)(1.66)10^{-5}\,(2)10^{-2}}{(2 \times 10^{-2})^2} = 1.66 \times 10^{-3}$$ or 1 part in 602 (for 5 arc seconds)
or 1 part in 301 (for 10 arc seconds)

where l = one side of the square image = 0.02 in.

**Fig. C-1 Basic Optical/Geometric Relationship for a Collimated Twist Sensor System**

For a maximum twist of 0.08° ($1.396 \times 10^{-3}$ rad), the pseudo-yaw motion in the image plane is given by $y = 2\rho(\sin\theta)FL$ (see Fig. C-1).

$$y_{max} = 9.3 \times 10^{-4} \text{ in.}$$

This does not affect the sizing of the prism.

FOCUSED SYSTEM

The basic geometry for a focused twist sensor system is shown in Fig. C-2. It is apparent that a focused system is simpler than the collimated. The image displacement within the twist angle receiver does not depend on the lens (receiver objective optic) focal length or on the ratio R/L as in a collimated design. However, the receiver image size is larger because of the magnification imposed by the focused transmitter optic. In order to maintain a reasonably sized received image, it is necessary to start with a smaller source aperture (see Fig. 7). The system magnification is the ratio of the distance of the projection (transmit) optic image to the distance of the source aperture. For a 4-in. FL projection optic and a boom length of 240 in., the magnification is 120. A source aperture of 0.010 $in^2$ is reduced in apparent size as seen by the projection lens by means of a negative intervening lens. A -6 mm lens results in a source aperture minification of 0.23. The total system magnification then is

$$M = M_1 M_2 \quad ,$$

where

$M_1$ = magnification of the negative lens, and

$M_2$ = magnification of projection optic.

Therefore

$$M = (0.23)(120) = 27.6 \quad .$$

The received image size, I, is the product of the magnification, M, and the source aperture size, or I = 0.276 in. The image is about 10 times larger than that of a collimated system. Correspondingly, the receiver prism splitter and the condenser optic must be larger.

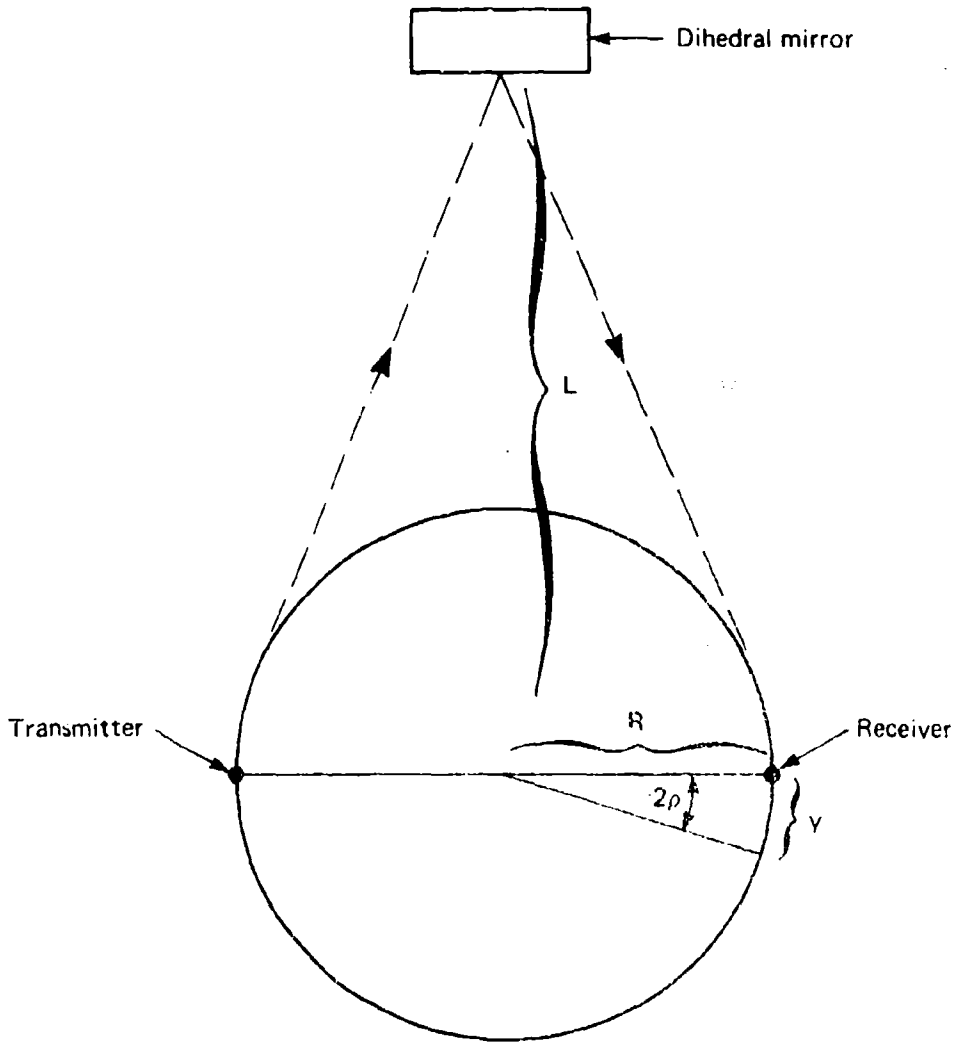


$y = 2\rho R$

If $\rho$ = 5 arc seconds = 25 $\mu$rad

R = 10 in.

$y = 5 \times 10^{-4}$ in.

y = twist image displacement (pseudo-yaw)

$\rho$ = twist angle

R = radius of transmitter/receiver base circle

**Fig. C-2 Basic Optical/Geometric Relationship for a Focused Twist Sensor System**

The prism splitter and the condenser optic sizes are governed by the image size and the effective pitch motion that must be handled along the roof line of the mirrored prism splitter (Fig. 7). For a pitch tolerance of ±3 arc minutes, the image motion in the twist receiver is

$$p = \pm PL$$

where

p = linear pitch motion in image plane, and

L = boom length.

If

L = 240 in.,

then

$$P = \pm 3 \text{ arc minutes} = 8.7 \times 10^{-4} \text{ rad},$$

$$= 0.209 \text{ in.}$$

Therefore the prism splitter must have a minimum length of 2p + image size = (2)(0.209) + 0.276 = 0.694 in. Likewise, the minimum effective diameter of the condenser optic must be this same value.

The pseudo-yaw motion in the image plane resulting from a maximum twist of ±0.08° = $1.396 \times 10^{-3}$ rad is

$$y = \pm 2\rho R = \pm(2)(1.396)10^{-3}(10) = \pm 0.0279 \text{ in.}$$

This is less than any image motion resulting from maximum allowable pitch and does not affect the sizing of the prism splitter or the condenser optic.

A 5-arc-second twist of the dihedral mirror fastened to the magnetometer instrument package results in an incremental change in signal (two detectors) of

$$\Delta = 2yI/I^2$$

where

y = image displacement due to twist ($5 \times 10^{-4}$ in.), and

I = one side of the square image (0.276 in.).

Therefore

$$\Delta = \frac{2(5 \times 10^{-4})}{0.276} = 3.62 \times 10^{-3}$$

or one part in 276. This compares favorably with the results calculated for a collimated system (Fig. C-1). Theoretically, either system will perform well. However, the practical aspects of maintaining the thermomechanical tolerances of the optical bench will determine the selection.

## DIHEDRAL MIRROR

Both the focused and the collimated designs have a dihedral mirror fastened to the magnetometer instrument package. The length of the mirror is governed by the pitch motion range over which twist is to be measured. Twist will only be measured when the pitch/yaw sensor is within its precision range of ±3 arc minutes; this corresponds to 0.418 in. for a 240-in. boom length. The minimum length of the mirror must therefore be the beam diameter plus 0.418 in. if vignetting parallel to the mirror roof line is to be avoided. The width of the mirror is governed by the size of the optical beam. In order to avoid beam translation effects induced by the mirror, it is necessary that the mirror be equal to or smaller than the diameter of the impinging beam for a focused system.

In a collimated system, only the angle of the reflected rays is of concern. The displacement of rays by the dihedral mirror is only significant if such displacement results in vignetting at the receiver objective optic. Beam vignetting at the mirror usually occurs in a focused system. If 3-dB signal vignetting is considered for a focused system at a yaw angle of ±3 arc minutes, the width of the mirror must be 0.418 in. This must also be the diameter of the optical beam at the mirror.

For a focused system, the dihedral mirror can be 0.418 in. wide by a minimum of 0.836 in. long. It must be remembered that rays at the mirror in a focused system are out of focus. By having the beam diameter equal to the width of the mirror, the vignetting is held to a minimum and beam translation effects are avoided. In the case of a collimated system, one must consider the tradeoff between using a smaller dihedral mirror to avoid vignetting and using a mirror larger than beam size, which will cause vignetting at the receiver objective optic. Figure C-3 illustrates the relationships between beam and dihedral mirror sizes.

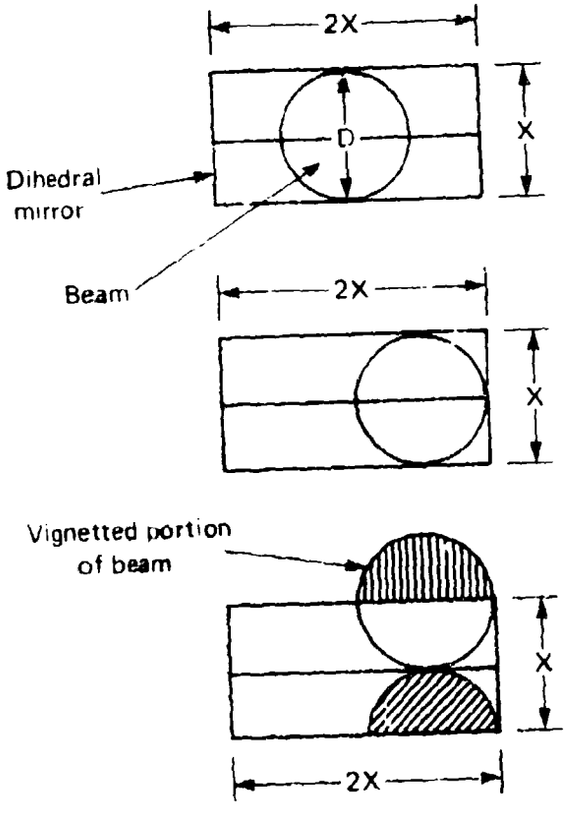


Boresight condition

Maximum pitch shift (3 arc minutes)

Maximum yaw (3 minutes) shift
and maximum pitch (3 arc minutes) shift

For focused system $D \geq X$

For collimated system $D \gtrsim X$

**Fig. C-3 Beam/Dihedral Mirror Geometry**

If the experiment platform is subject to a lateral displacement equivalent to 0.25° at a boom length of 240 in. while the pitch/yaw system and its flat mirror are in the precision measurement range of ±3 arc minutes, the dihedral mirror is also subject to an equivalent ±0.25° lateral displacement. This means that the mirror must be large enough to cope with such a situation, i.e., 2 in. wide by 4 in. long. For a focused twist sensor, the beam would have to be large, i.e., 2 in. in diameter. For a collimated system, the beam could have the 0.418-in. diameter discussed above; the dihedral mirror would be 2.5 $in^2$.

## TRANSMITTER PROJECTION OPTIC

For a collimated system, the transmitter projection optic should have a diameter equivalent to the desired beam diameter at the dihedral mirror, which in the above case was 0.418 in. For an 8-in. focal length, this is an f/19 system.

For a focused system, a transmitter projection optic diameter of 0.56 in. (f/7) is desired for a beam size of 0.418 in. at the dihedral mirror and an image size of 0.276 in. However this is only when the mirror is in a position of zero translation with a maximum pitch or yaw angle of ±3 arc minutes. If ±0.25° translation prevails, a 2-in. beam diameter is required at the mirror, which means a projection optic with a diameter of 3.72 in. (f/1 for 4-in. FL).

## RECEIVER OBJECTIVE OPTIC (COLLIMATED SYSTEM ONLY)

The focal length of the receiver objective optic should be the same as the diameter of the transmitter projection lens, provided the image size is to be identical to that of the transmitter source aperture. The diameter of the receiver objective optic is determined by the diameter of the collimated beam plus the lateral excursion range imposed by the pitch/yaw precision dynamic range. In the more severe case, ±0.25° imposed by boom/experiment package translation, the 0.418-in. ray bundle could experience a maximum lateral excursion of ±1 in., and a minimum lens diameter of 2.5 in. is necessary.